Electron Accepting Perylene Dyes with Versatile Imide Substituents: Synthesis and Characterization

Safa Elshreef Eltabeb

Submitted to the
Institute of Graduate Studies and Research
in partial fulfillment of the requirements for the Degree of

Master of Science
in
Chemistry

Eastern Mediterranean University
February 2015
Gazimağusa, North Cyprus

Approval of the Institute of Graduate Studies and Research

Prof. Dr. Serhan Çiftçioğlu
Acting Director

I certify that this thesis satisfies the requirements as a thesis for the degree of Master of Science in Chemistry.

Prof. Dr. Mustafa Halilsoy
Chair, Department of Chemistry

We certify that we have read this thesis and that in our opinion it is fully adequate in scope and quality as a thesis for the degree of Master of Science in Chemistry.

Prof. Dr. Huriye İcil
Supervisor

Examining Committee

1. Prof. Dr. Huriye İcil

2. Asst. Prof. Dr. Jagadeesh Babu Bodapati

3. Asst. Prof. Dr. Hürmüs Refiker

ABSTRACT

Perylene bisimides (PBIs) have received significant attention due to their exceptional photophysical and optical properties. Derivatives of PBIs show high fluorescence quantum yields, high electron affinities and large band-gaps, that make them excellent candidates for numerous optoelectronic devices such as light-emitting diodes, photovoltaics, optical switching, and electroluminescent devices. PBIs are considered as *n*-type semiconductors in which the main charge carriers are in their conduction band. On the other hand, most organic conducting substances are *p*-type semiconductors.

In the current work, the synthesis of a new perylene bisimide N,N′-Bis(1-methyl-2-cyanoethene**)**-3,4,9,10-perylenebis(dicarboxiimide) (EAPDI) was carried out. 1-methyl-2-cyanoethene substituent is specifically chosen so that the imide regions of perylene core offer better solubility and impressive optical properties of the perylene bisimide. The synthesized bisimide was approved by FT-IR and its photo-physical properties were studied by UV–vis and emission techniques.

EAPDI has high molar absorptivity as well as high fluorescence quantum yields (Φ_f = 0.72). The absorption and emission spectra of EAPDI are mirrored images in DMF, $CHCl_3$, MeOH with smaller Stoke shifts.

Keywords: Perylene bisimide, 1-methyl-2-cyanoethene, absorbance, fluorescence.

ÖZ

Perylenebisimide'ler (PBIs) olağanüstü fotofiziksel ve optik özellikleri nedeniyle önemli ilgi görmüştür. PBIs Türevleri, yüksek floresan kuantum verimleri, yüksek elektron ilgileri ve geniş band aralıkları göstermekte, bu özellikler onları ışık yayan diyotlar, fotovoltaikler, optik anahtarlama, ve elektrolüminesans cihazlar gibi çok sayıda optoelektronik cihazlar için mükemmel adaylardır yapmak. PBI'ler ana yük taşıyıcıların iletkenlik bandında olmasından dolayı *n*-tipi yarı iletken olarak kabuledilmektedir. Diğer yandan, birçok organik iletken maddeler *p*-tipi yarı iletkenlerdir.

Mevcut çalışmada, yeni bir perylen bisimid N,N'-Bis(1-metil-2-siyanoeten)-3,4,9,10-perilen bis(dikarboksimid) (EAPDI) sentezi gerçekleştirilmiştir. Sübstitüe 1-metil-2-siyanoetenperilenin imid bölgelerine bağlanarak daha iyi bir çözünürlük sunmaktadır ve perilen bisimidin optik özellikleri etkileyicidir. Sentezlenen bisimid,FT-IR ile kanıtlanmış ve bunun foto-fizikselözellikleri UV-Vis ve emisyon teknikleri ile çalışılmıştır.

EAPDI, yüksek molar absorplama yanında yüksek floresan kuantum verimine(Φ_f = 0.72) sahiptir. EAPDI'in absorpsiyon ve emisyon spektrumlarıküçük Stoke kaymaları ile DMF, $CHCI_3$, MeOH'da ayna görüntüsündedir.

Anahtar: Perylenebisimid, 1-metil-2-siyanoeten, absorpsiyon, floresan.

To My Family

ACKNOWLEDGMENT

Firstly, I would like to thank my supervisor Prof. Dr. Huriye İcil for her kindness and close follow up throughout my study in general and this research in particular. I am very grateful to her for giving such an education in every aspect.

Also, I thank Dr. Duygu Uzun who helped me to accomplish this study. Her kind advice and comments have made this research a rich experience for me.

Additionally, I would like to express my gratitude to all my instructors who encouraged me to learn and to realize the value of scholarship.

To the virtuous Dr. Mohamed Ayiad Grebee.

To my lovely parents.

To my sister Dr. Maisa who accompanied me and helped me during my residence in Cyprus.

TABLE OF CONTENTS

LIST OF TABLES

LIST OF FIGURES

LIST OF ILLUSTRATIONS

LIST OF ABBREVIATIONS

$\overset{o}{A}$	Armstrong
A	Absorption
Abs	Absorption
KBr	Potassium bromide
EAPDI	N,N′-Bis(1-methyl-2-cyanoethene**)**-3,4,9,10-perylene bis(dicarboxiimide)
AU	Arbitrary unit
DSSCs	Dye-sensitized solar cells
Cm	Centimeter
c	Concentration
DMF	N,N′-dimethylformamide
ε	Molar Extinction/Absorption coefficient
ε_{max}	Molar Extinction coefficient/Molar absorptivity
E_g	Band gap energy
E_s	Singlet energy
τ_0	Theoretical radiative lifetime
τ_f	Fluorescence lifetime
k_f	Fluorescence rate constant
Φ_f	Fluorescence quantum yield
f	Oscillator strength
FT-IR	Fourier transform infrared spectroscopy
g	gram

h	Hour
HOMO	Highest occupied molecular orbital
IR	Infrared
^{o}C	Degrees celcius
kcal	Kilocalorie
l	Cell length
LUMO	Lowest unoccupied molecular orbital
M	Molar concentration
max	Maximum
mol	Mole
mp	Melting point
UV	Ultraviolet
UV-vis	Ultraviolet and visible light absorption
$\bar{\nu}$	Wavenumber
$\Delta\bar{\nu}_{1/2}$	Half-width (of the selected absorption)
$\bar{\nu}_{max}$	Maximum wavenumber/Mean frequency
V	Volt
λ	Wavelength
λ_{exc}	Excitation wavelength
λ_{em}	Emission wavelength
λ_{max}	Maximum wavelength

Chapter 1

INTRODUCTION

Derivatives of perylene diimide are colorants which are extensively analyzed in industrial pigments and dyes. Previously, the mother compound of these categories of dyes was discovered and named as perylene-3,4,9,10-tetracarboxylic dianhydride which is abbreviated as PTCDA [21]. Modification can be done on the imide group or at the bay position with various types of substituents to give diverse classes of perylene bisimides (PBIs). Figure 1.1 below illustrates the chemical structures of PTCDA and PBIs, respectively.

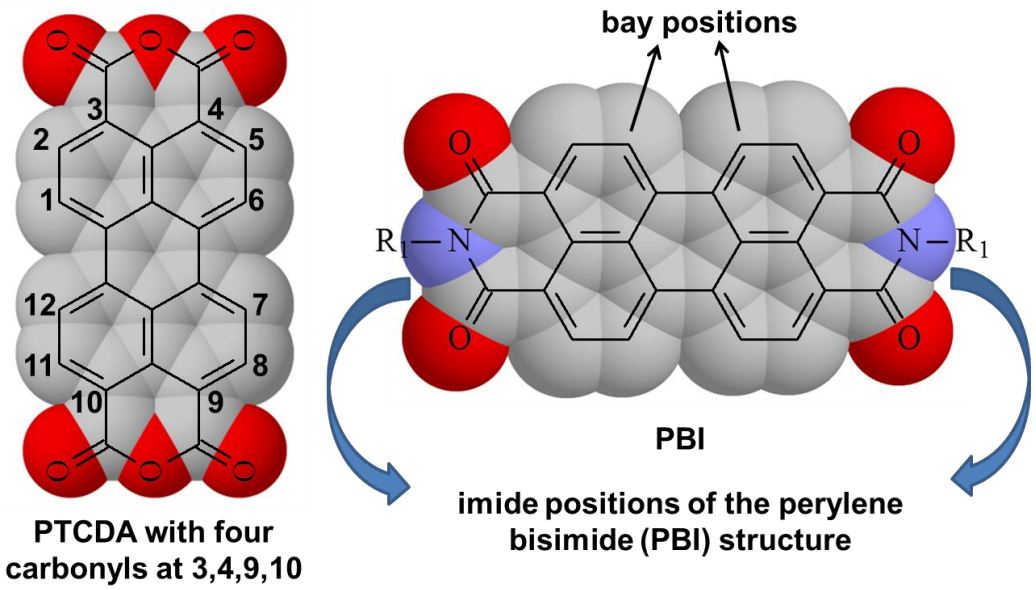

Figure 1.1: Basic Structures of Perylene Family – A Perylene Dianhydride (PTCDA) and a Perylene Bisimide (PBI)

PBIs with carboxylic groups show a special combination of redox and electro-optical characteristics. They possess high stabilities and are largely employed in devices of

organic-electronics as *n*-type materials especially in field effect transistors, display of liquid crystals, solar cells, light harvesting substances, light-emitting diodes, photodynamic therapies, chemo-sensors. It is important to note, numerous synthesized dyes exhibit lower solubility in organic solvents. This creates a hindrance to their synthesis and applications in material science. The solubility can be improved by long alkyl/alkoxy-substitutions at the dye's imide positions (N-positions). The high stability of PBIs originates from huge resonance energy and π-π interactions as a result of planar molecular design of PBIs. They also show huge and sharp peaks of absorption at around 530 nm [5–8].

PDI dyes are widely applied in organic photovoltaics (OPVs). Photoelectric conversion in organic solar cells (OSC) solely relies on processes of transfering photo-induced electrons which require two semiconducting substances possessing different electron affinities and potentials of ionization. This constitutes a bulk hetero-junction (BHJ) device. BHJ active layers are bi-continuous interwoven networks composed of an electron-rich and electron-deficient materials. Usually, a π-conjugated molecule and an electron withdrawing derivatives are employed [9–11].

PBIs are some common organic dyes that used in dye-sensitized solar cells. However, there are many disadvantages of these organic dyes such as: the lack of light absorbance at red and NIR regions, the unsuitable position of the LUMO level, high aggregates and low solubility [6].

In this research work, we design and synthesize a new perylene bisimide derivative (EAPDI) with strong electron with drawing groups introduced at the imide nitrogen (Figure 1.2). It is expected that perylene bisimide EAPDI with cyanide groups could possess strong electron accepting nature as the perylene chromophore itself is electron acceptor with four carbonyl groups. The synthesized compound was investigated in detail by the spectroscopic techniques – UV-vis, emission, and FTIR.

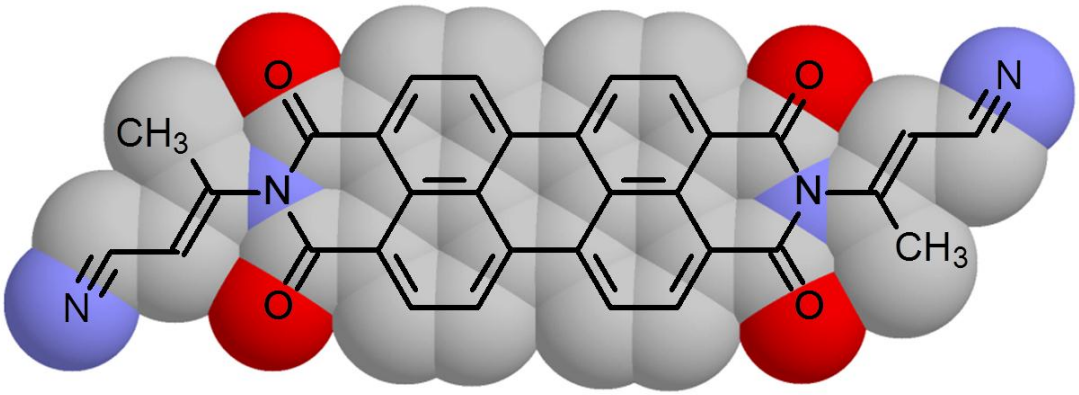

Figure 1.2: The Synthesized Perylene Bisimide Dye, EAPDI

Chapter 2

THEORETICAL

2.1 General Properties of Perylene Dyes

Perylene dyes have taken attention with potential applications in electronic devices like organic field effect transistors (OFETs) and photovoltaic cells. The main advantages of these dyes are their high thermal, physical and optical stability. Moreover, they have excellent fluorescence quantum yields and high molar extinction coefficients. However, always it is not so easy to duduce all these extraordinary characteristics of perylene derivatives due to their restricted solubilities. Mostly, they show moderate to complete solubilities in high dielectric constant-dipolar aprotic solvents [8–11]. Utmost care should be taken concerning the design of perylene derivatives if they are aimed for various opto-electronic applications as processability plays key role in exploring their potential applicabilities [21–11].

2.1.1 Optical Properties of Perylene Dyes

As mentioned earlier, perylene derivatives exhibit excellent opto-electronic properties like large absorption in the visible to infrared spectral range, quantum yield of fluorescence near to one, and tunable low electrochemical band-gaps [2–11].

Different conditions and parameters can affect the opto-electronic properties of the perylene derivatives such as type of substituent with key functional groups that attached to perylene derivatives at various positions and the length and bulkiness of

the substituents. However, the efficiencies of DSSCs that employed perylene dyes were enhanced with increase in the chain length of the substituent [1–2].

Another important factor is the substitution position of the substituent which possesses various functional groups. Perylene chromophore has several positions where the substituents can be attached. Attached at the bay- or core-, imide- and peri-positions of the perylene chromophore, perylene chromophoric dyes exhibit versatile opto-electronic properties. The wavelength of absorption for bay- or core-substituted perylene derivatives is usually longer than that of imide- and peri-substituted perylene dyes [18]. The structure illustrating substitution patterns of perylene chromophore is shown below (Figure 2.1).

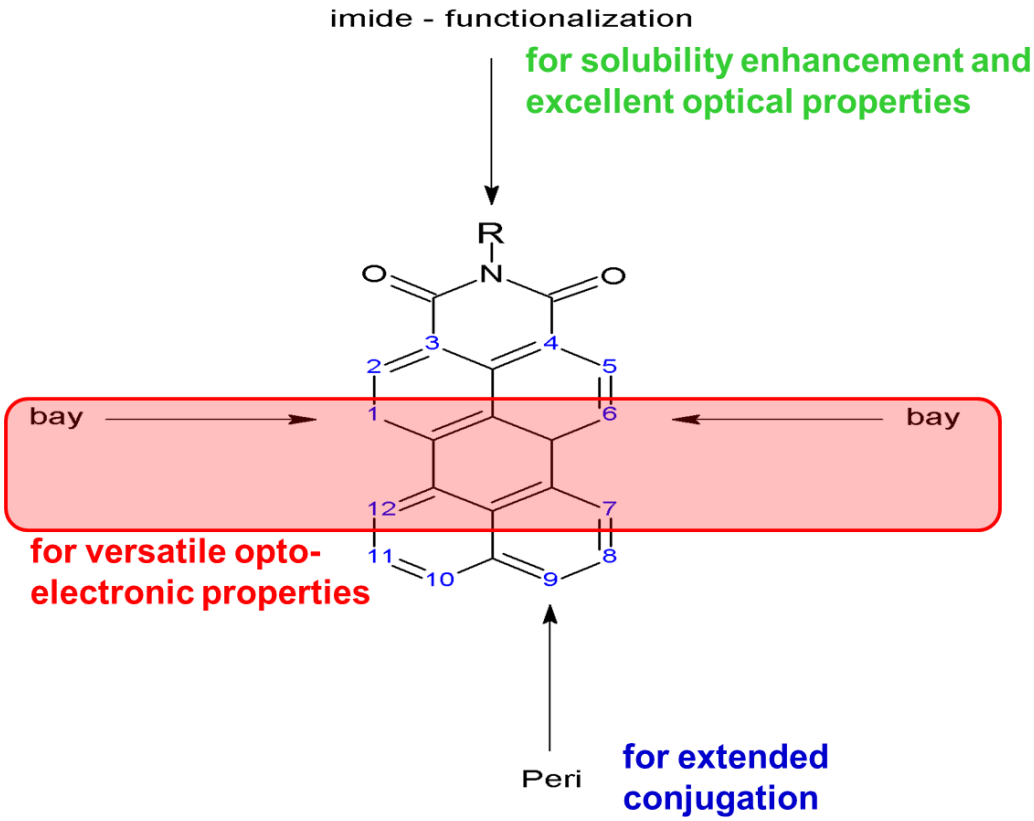

Figure 2.1: The Structure Illustrating Substitution Patterns of Perylene Chromophore

2.1.2 Electron Acceptor Properties of Perylene Dyes

Perylene derivatives are well known as excellent electron acceptors as they possess four carbonyls (shown representatively in Figure 1.1). The carbonyl groups are well known for their electron accepting property. Together with the conjugation of perylene chromophore, the carbonyls readily accept the electrons and form a monoanion. Further, they accept one more electron to form a dianion. Generally, the perylene dyes accept two electrons and form finally a dianion. When the electron accepting or electron withdrawing substituents are attached to the perylene chromophore, they accept the electrons more readily and they could be used semiconductors (with *n*-type semiconducting property) in organic solar cell construction [14–16].

2.2 Substituent Effects on Perylene Dyes

2.2.1 Functionalization of Perylene Dyes with Different Substitution

Perylene dyes could be constructed by attaching a vast variety of groups with versatile functional groups depending on the purpose. Generally, the choice is made to improve their solubility, absorbance capacities, light-emitting (by delivering photons) abilities and band gap energies [5, 14, 16–21].

The effect of attached substituents on the electronic properties is mostly apparent when they are attached at bay- or core-positions of the perylene chromophore. However, when long chain alkyl substitutions bonded at the bay positions of perylene chromophore, the dye exhibits generally electron donating properties. On the other hand, substitution of groups who can extend conjugation and electron withdrawing nature could result in enhanced electron accepting nature of perylene dyes. Therefore, perylene dyes with suitable substituents could act as both electron

donors and acceptors which make them superior over other conjugated aromatic dyes. However, the substituted perylene dyes build an electron acceptor-donor system where the intramolecular charge transfer occurs by push-pull process because of the conjugation of the π-system between the donor and acceptor [13, 16].

Perylene dyes can be absorbing at the NIR by functionalization it at bay positions. For example, the functionalization of perylene cyclohexyldiimide derivative with piperidinyl groups at 1-, 6- and 1-, 7-positions, make them to have maximum absorptions at around 650–700 nm [13].

In the literature, so many perylene dyes were reported with different alkyl chain substitutions. After that, the properties of photophysics and electrochemistry of each prepared dye were investigated and compared with each other. The few synthesized materials were shown in Figure 2.2 [6,8,10,11,13]. However, so many aromatic substiuent attached perylene dyes were also reported with outstanding opto-electronic properties.

The alkyl chains are generally brought for higher solubility. Especially branched alkyl chains are reported as excellent substituents to enhance the solubility of these rigid aromatic perylene chromophoric derivatives (Figure 2.2).

Similar perylene family dyes with extended conjugation were used for higher absorption of electromagnetic radiaton and hence to be used for photovoltaics.

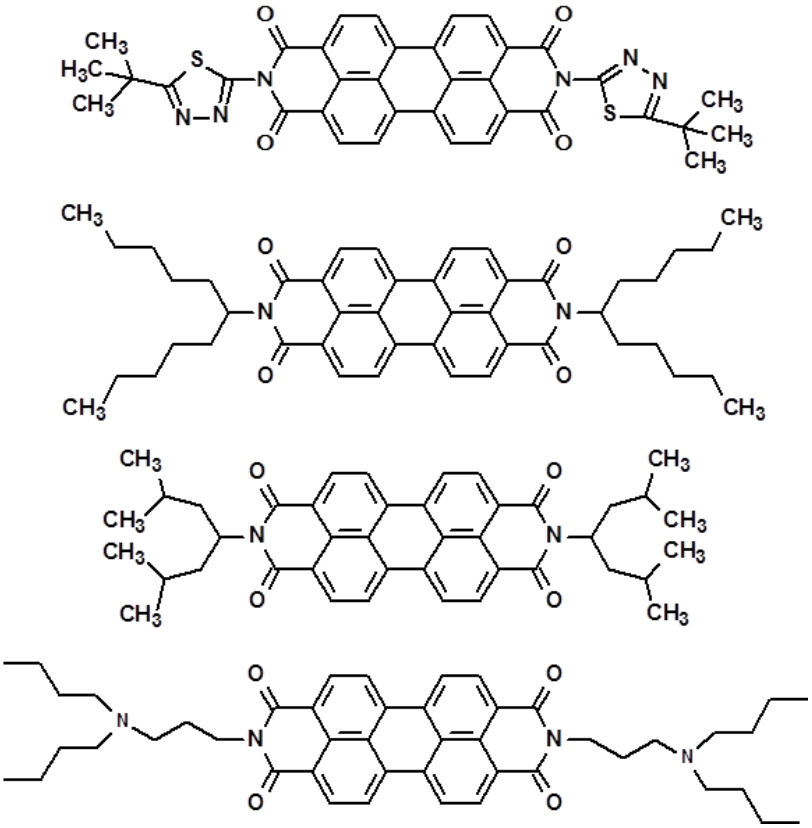

Figure 2.2: The Structural Models of Perylene Bisimides with Different Alkyl Chain Substituents [6,8,10,11,13]

The remarkable opto-electronic properties are not only due to the intermolecular interactions but also possible with intramolecular interactions. Intramolecular charge transfer characteristics of dyes are being altered by the presence of functional group species as substituents of perylene core. Comparing to the intramolecular charge transfer resulting from peri-positions of the perylene core, perylene bay-position substituted monoimide and diimide dyes with the same functional species show a higher intramolecular charge transfer character [16].

2.2.2 Electron Donor Substituent Effects on Perylene Dyes

The efficiency of perylene dyes that used in DSSCs can be depending on the electron donating or accepting strength of the substituents. However, the electron donor can be attached to imide group of perylene derivatives while in recent years it can be attached to the bay position using conjugated linkers. Chao *et al.* reported that

hypochromic shifts of the maximum absorptions occur when the ability of electron donating substituent increases. However, the photophysical and electrochemical properties could be affected by the strength of electron donating substituent. For example, 1,7-diaryl-substitutedperylene diimides (1,7-Ar_2PDIs) were reported previously with different aryl (Ar) substituents and their photophysical and electrochemical properties were determined. The structure of the reported compounds were shown in Figure 2.3 [17].

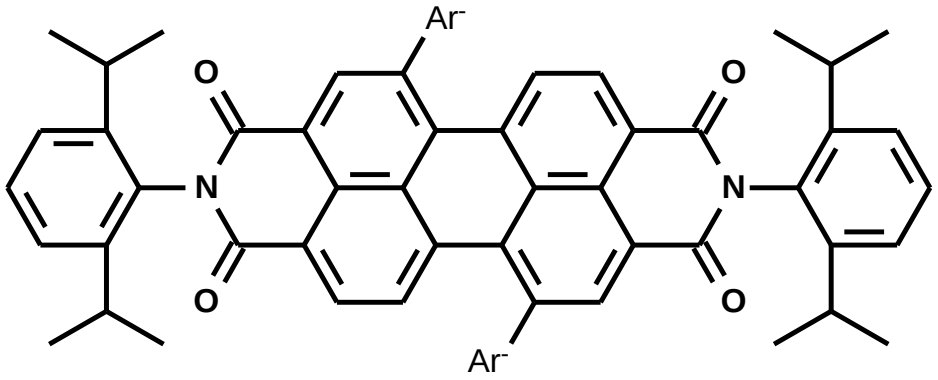

Figure 2.3: The Structure of 1,7-Ar_2PDIs with Different Aromatic Substituents [17]
Ar = mesityl, 4-$MeOC_6H_4$, 1-naphthyl, 2,4-$(MeO)_2C_6H_3$, phenyl, 2,5-$(MeO)_2C_6H_3$, 4-PhC_6H_4, 4-$Ph_2NC_6H_4$, 4-$CHOC_6H_4$

According to the previously reported results, it could be generalized that the electron donating ability of various substituent-attached perylene derivatives. Specifically, the electron donating ability of perylene monoimide acquiring an aromatic substituent (Ar-PMI) is more higher than that of perylene monoimide with cyclohexyl substituent (cyclohexyl-PMI). This could be explained by the higher electron density of Ar-PMI derivative than that of cyclohexyl-PMI. Therefore, the electron injection from Ar-PMI to the semiconductor (of the photovoltaic architecture) could be better than that of cyclohexyl-PMI [4, 22]. The structures of the Ar-PMI and cyclohexyl-PMI were representatively shown in Figure 2. 4 [4, 22].

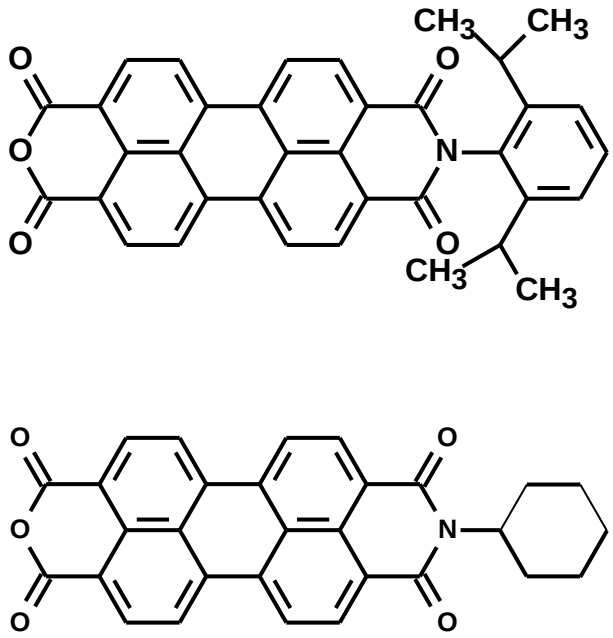

Figure 2.4: The Structure of Ar-PMI (top) and Cyclohexyl-PMI (bottom) [4, 22]

2.2.3 Electron Acceptor Substituent Effects on Perylene Dyes

One of the most important electron acceptor-substituents known is fullerene and its derivatives. But, the most disadvantage concerning these compounds is their poor absorption in the visible range. The attachment of fullerenes to PBIs was carried out at the imide positions previously. However, the electron transfer from PBIs to fullerenes occur in polar solvents, generally. In polar solvents, it was reported that the PBI-C_{60} system could exhibit excellent absorption properties in the NIR and visible light region [19]. The structure of PBI-C_{60} system that has been reported previously was representatively shown in Figure 2.5.

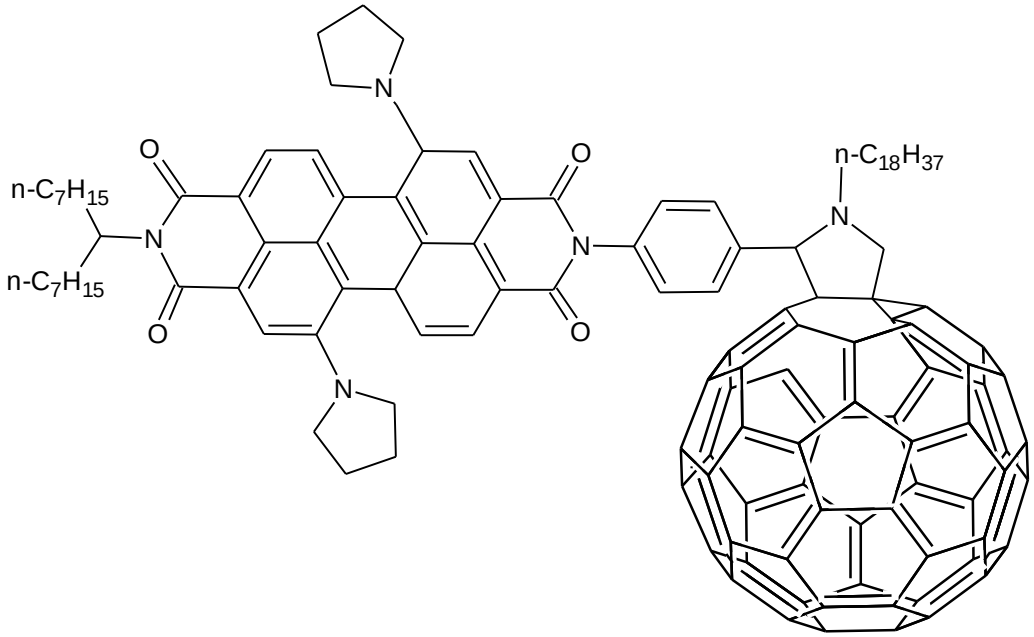

Figure 2.5: The Structure of PBI-C_{60} System [19]

However, the PBI shown in Figure 2.5 could be used as electron donor by functionalizing it with pyrom ellitimide and naphthalene diimide substituents at the imide position. The electron transfer using these substituents can be occurred in polar and nonpolar solvents [1, 14].

2.3 Solar Cell Concepts

The principle of solar cell is the conversion of solar light into electrical energy using photovoltaic effect. The interest in construction of solar cells is because their potential applications considering renewable and clean source energy. The inorganic composite-material (such as semiconducting multi-crystalline silicon, Gallium Arsenide) made solar cells are commercially famous in today's technology [7–15]. Multi-crystallines, amorphous and single crystalline categories are often used nowadays as PVs for solar energy grids [4]. However, their performance and cost are directly proportional as highly pure silicon is employed for better efficiencies.

Another challenge to these model designs to possess a very long term stability. Commercially, chemical constances are the main issues of concern.

In order to bring out a solution for cost-effective efficient solar cells, organic material-based solar cells come into the limelight of potential renewable energy sources. Organic materials used in solar cells applications must have additional properties as to their inorganic counterparts. As mentioned earlier, the absorbance range of light wavelength is narrow for semiconductors due to their wide band gaps. Dyes can be used to improve the light absorbance range so that the solar cells can employ these electron-donating or accepting dyes. Dye-sensitized solar cells are reviewed as most promising and efficient renewable energy resources of future. However, the dye can be absorb photons at visible and near infrared (NIR) regions from the sunlight. After that the photoexcited electrons were injected into the band gap of the dyed semiconductor such as TiO_2 nanoparticles. The advantages of these cells are the high efficiency, flexibility and low cost [8].

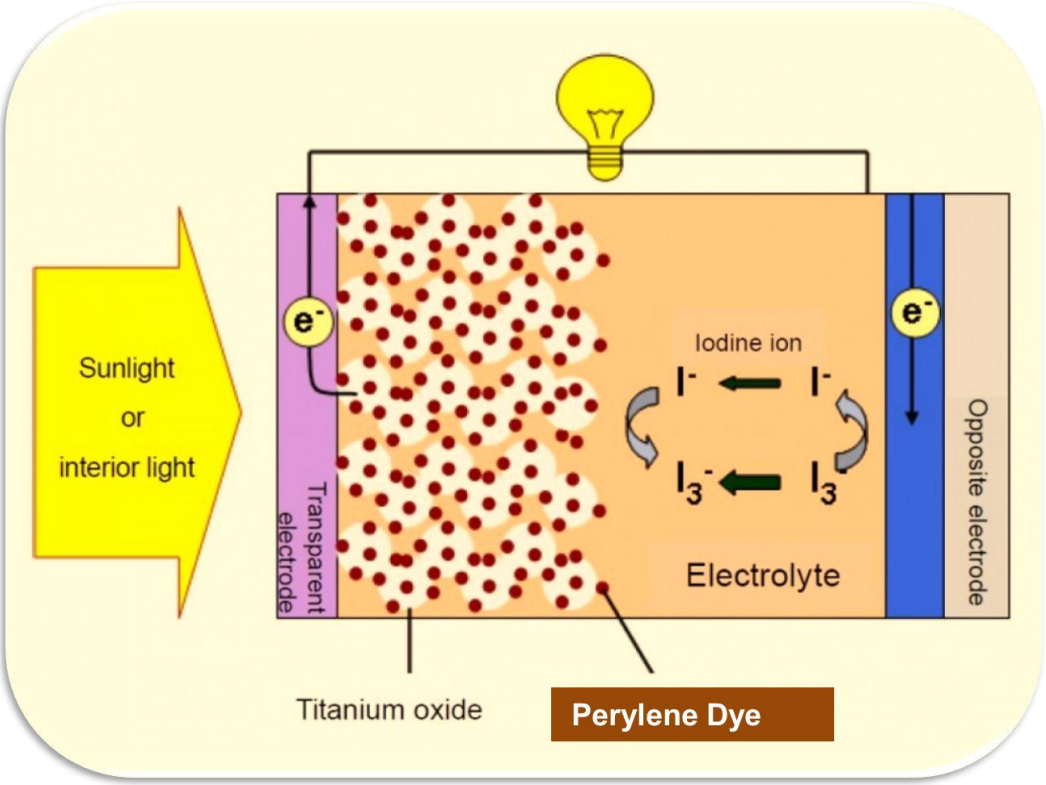

Figure 2.6: General Mechanism of a DSSC Employing Perylene Dyes

This way of converting energy is mimicking photosynthesis and could be called as artificial photosynthesis of light harvesting (Figure 2.6). However, the efficiencies of organic-material based DSSCs are not as impressive as amorphous material based solar cells. There are many parameters that need to be optimized for efficiencies higher than amorphous-material based solar cells as well as for fruitful efficiencies at lower cost. It is certain that amorphous materials usually offer wider band gaps when compared to organic materials. This made the amorphous materials restrict to narrow wavelength and frequency range of absorption. On the other hand, organic materials could offer wider range of absorption wavelengths. Another attractive point regarding these organic-based materials is their environmental friendly nature of producing and processing when compared to their inorganic counter parts. The applicability onto larger surfaces gives them an additional advantages. Flexibilities are increased on batteries and these widen its scopes of application. OPVs have been

modified by synthesizing these substances with higher attributes from different species of reagents and reactants. Conjugated polymer is being used as PVs as a result of their higher molar absorption coefficients [4]. This is the motivation for researchers to go for synthesizing numerous organic materials which could apt for DSSCs so that the problems might overcome and reach higher efficiencies at lower cost.

2.4 Applications of Perylene Dyes

As reported in the previous section, DSSCs consists of organic-dye semiconductors are much more fruitful than DSSCs that employ metals such as ruthenium. However, the organic-dyes which were employed in DSSCs possess conjugation, high molar absorptivities, etc. Therefore, perylene dyes and its derivatives best fit into the category and in literature, successfully reported many DSSCs with appreciable efficiencies [8].

2.4.1 Perylene Dyes in Dye Sensitized Solar Cells

The molar absorption coefficients in long wavelength range, chemical, thermal and photophysical stabilities of perylene dyes enable them to be an efficient dye used in DSSC applications. However, designing TiO_2-DSSC structure based on perylene-imide derivatives is a great deal. The efficiencies reached from this combination is not so fruitful till date. This explains the challenges hidden in the design and optimization of set of parameters [3,12,22]. In addition, organic substances are predicted to illustrate higher degrees of environmental stabilities since the environment is composed of diverse abnormalities such as sunshine, oxygen, excessive rains, heat, and dust.

The key point about perylene derivatives is the easiness in preparation with a very wide variety of functional group substituents. This tailor made preparation leads to have a

number of perylene dyes with variety of properties. This makes them useful to optimize and modify accordingly [12].

2.4.2 Perylene Dyes in Molecular Devices

The stability of perylene is one of the most advantage properties for used in the molecular electronics field [10]. Majority of molecular appliances is made up of π-π interactions particularly phthalocyanines. Zinc phthalocyanine perylene diimide ($ZnpCIm_4$- PDI $_4$) derivatives covalently bonded results in self-assembly. This gives rise to the production of extensive fibrous designs in which adjacent covalent building blocks made up of sub-units of PDI stacks with those of $ZnpCIm_4$. In this way, ultra transfers of energies occur from the peripheral aggregates of PBI chromophores to the core of the aggregated $ZnpCIm_4$. Migration of excitons succeeds this between chromophores of $ZnpCIm_4$ in a very brief time interval.

Another application that has been reported recently is in the metallo supramolecular squares which functions as an artificial complexes for cycling of light harvesters in purple bacterium. 4-dimethylamino-1, 8-naphthalimide fluorescence dye is binded to the bay positions of the chromophores of N'N-bispyridyl perylene diimide. These ditopic ligands undergoes self-assemblies controlled by coordinations of metal ions. This leads to multichromophores fluorescent scaffold squares incorporated with sixthteen dimethyl aminonaphthalimide antenna dyes and four core PDI dyes. Ninety-five percent energy transfer from dimethylaminonaphthalimide to the core of perylene from the absorption [20].

Chapter 3

EXPERIMENTAL SECTION

3.1 Materials

The basic raw material, perylene-3,4,9,10-tetracarboxylic acid dianhydride was obtained from FLUKA; whereas other reagents, 3-aminocrotononitrile, isoquinoline, *m*-cresol, and zinc acetate were obtained from ALDRICH.

The common organic solvents such as acetone and ethanol were obtained from SIGMA ALDRICH and were distilled according to the standard literature procedures.

3.2 Instrumentation

Infrared Spectra

The IR spectra were recorded on a JASCO FT-IR spectrophotometer by using solid state potassium bromide pellets.

Ultraviolet (Uv-vis) Absorption Spectra

The UV-vis absorption spectra were measured with Varian Cary-100 spectrophotometer.

Fluorescence/ Emission Spectra

The Fluorescence/ emission spectra were measured by using Varian-Cary Eclipse spectrophotometer.

3.3 Synthetic Method for perylenebis(dicarboxiimide) (EAPDI)

This study seeks to design and synthesize of a new perylene bisimide electron accepter for solar cell applications. For this purpose, the N,N′-bis(1-methyl-2-cyanoethene**)**-3,4,9,10-perylenebis(dicarboxiimide) (EAPDI) was synthesized successfully in one step.

The generally found reaction for the synthesis of N,N′-Bis(1-methyl-2-cyanoethene**)**-3,4,9,10-perylenebis(dicarboxiimide) (EAPDI) is shown in Scheme 3.1.

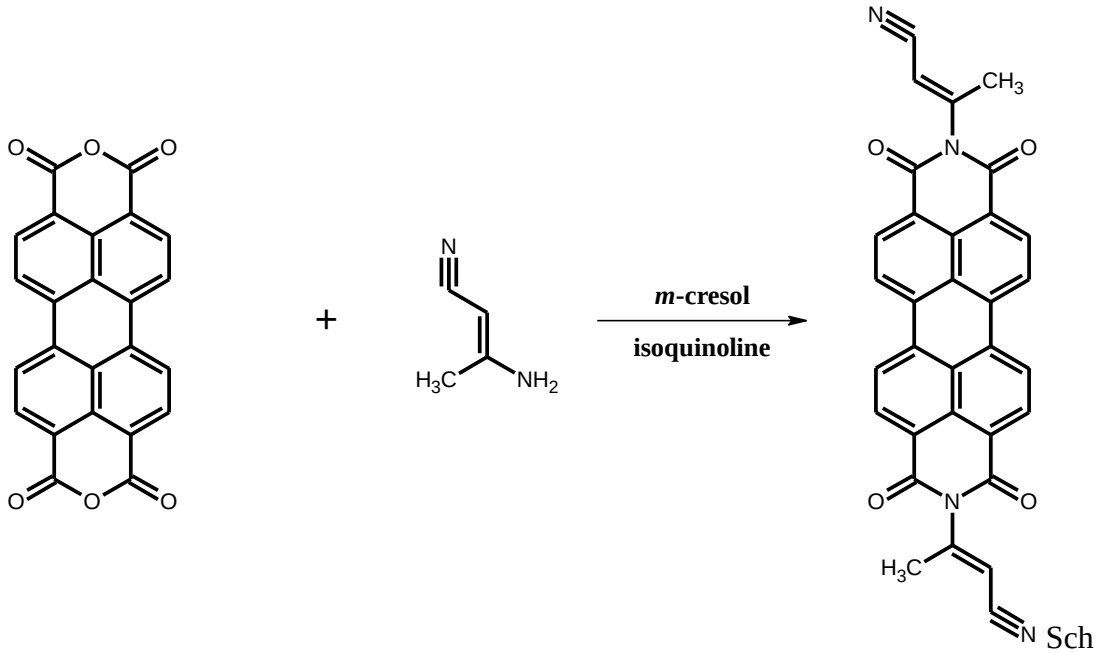

Sch

Scheme 3.1: Synthesis of N,N′-Bis(1-methyl-2-cyanoethene**)**-3,4,9,10-perylene bis(dicarboxiimide) **(**EAPDI).

3.4 Synthesis of N,N′-Bis(1-methyl-2-cyanoethene)-3,4,9,10-perylene bis(dicarboxiimide) (EAPDI)

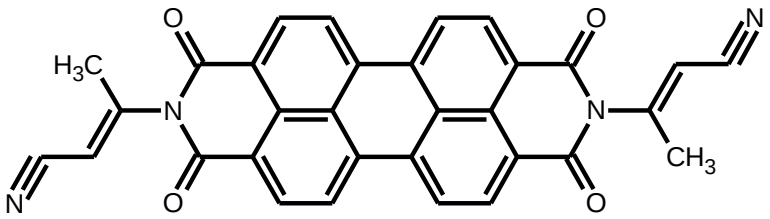

A mixture of perylene-3,4,9,10-tetracarboxylic acid dianhydride (1.013 g, 0.0026 mol) , 3-aminocrotononitrile (0.526 g, 0.0064 mol), zinc acetate (0.526 g, 0.0026 mol), *m*-cresol (40 mL) and isoquinoline (4 mL) were stirred under argon atmosphere. The reaction mixture was heated at 80º C for 1 hour, at 120º C for 1 hour, at 150º C for 2 hours, at 180º C for 3 hours and finally was heated at 200º C for 3 hours with good stirring. Then, poured the resulting solution into a 250 mL of acetone to obtain a precipitate. The precipitate is separated from the solution by suction filtration and purified by ethanol Soxhlet for 20 hours. The pure product dried at 100 º C in vacuum oven for 24 hours.

Yield: 82.3% (1.105 g)**, Color :** Black-brown.

FT-IR (KBr, cm^{-1}) : ν = 3438, 3057, 2855, 1698, 1657, 1592, 1274, 810, 744.

UV-Vis ($CHCl_3$) (λ_{max}/nm; (ε_{max}/ L mol^{-1} cm^{-1}) : 457 (39000), 490 (72000), 526 (92000).

Emission (DMF) (λ_{max}/nm) : 537, 574, 624; Φ_f = 0.72

3.5 Reaction Mechanism of Electron Accepting Perylene Dye

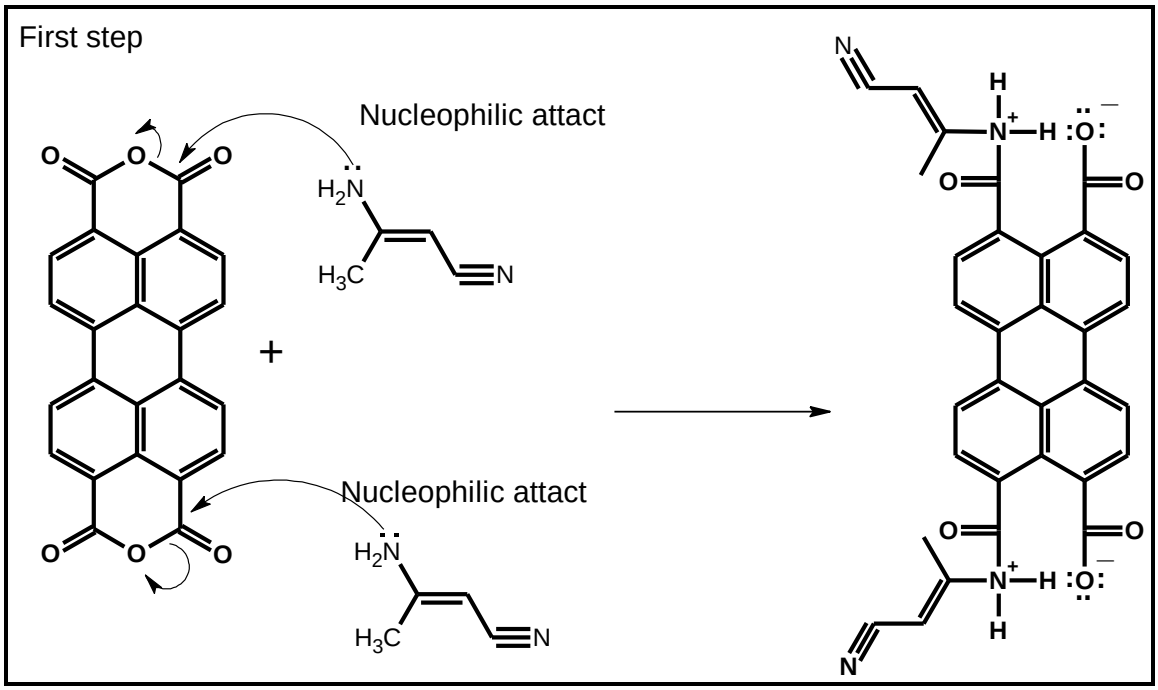

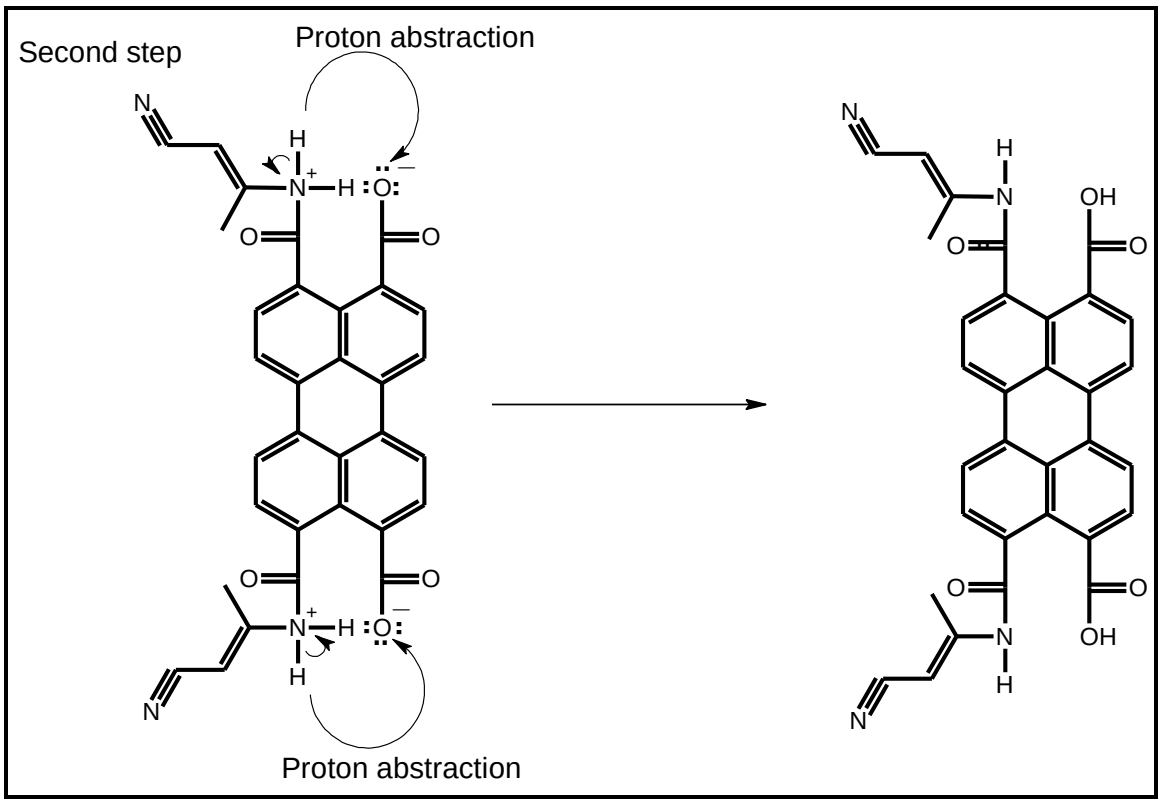

Third step

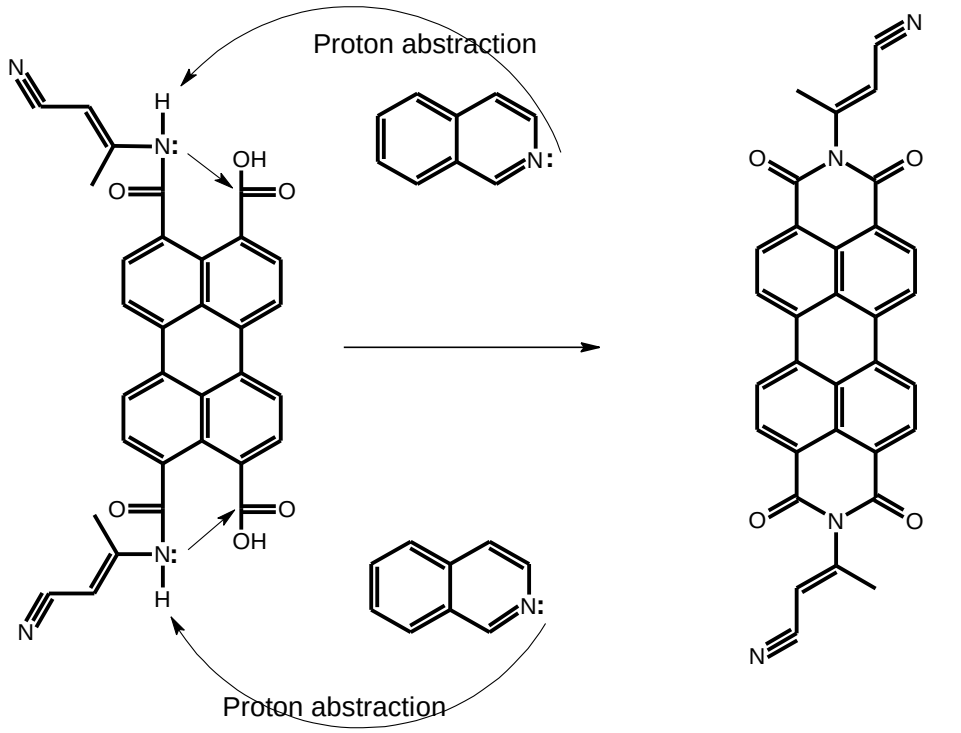

Fourth step

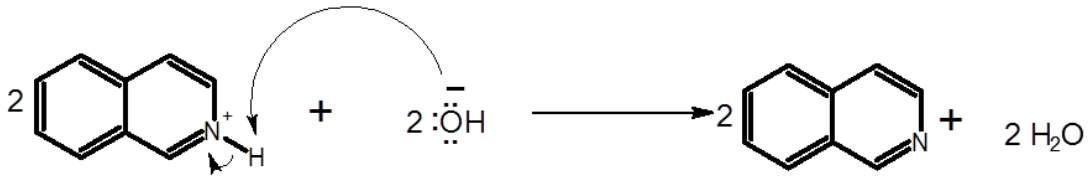

Chapter 4

DATA AND CALCULATIONS

4.1 Calculations of Fluorescence Quantum Yield (Φ_f)

When an amount of energy will be absorbed by a fluorophore from the light's electromagnetic radiaton, a dynamically operating state will start formulating. In midest of numerous deactivation energy operations, essentially, fluorescence is the radiative procedure that places the energy deactivation over emitting a photon. Heretofore, the probability of the previous process subjects the fluorophore and the nearby environment. Yet, the deactivation process is the utmost outcome and the molecules compulsoty turn back to the original state. There are few light/photon emitting and heat delivering deactivation processes like fluorescence, vibrational relaxation, internal conversion, and intersystem crossing, etc.

Fluorescence is one of the examples of photoluminescence where the light is emitted by the substance after exciting it at a particular wavelength. In this process, the light emission is carried out by releasing photons.

The quantum yield of perylene dyes is referred as fluorescence quantum yield as these dyes mainly fluoresces. The fluorescence quantum efficiency (Φ_f) could be estimated from the ratio of photons absorbed to photons emitted. Williams's et al comparative method is the most consistent process to footage Φ_f, this method employs well categorized regular specimens. Essentially, standard testing specimens

solution that retain equivalent volume of absorbance in the same activated wavelength taken into consideration absorbing equivalent quantity of photons. The ratio combination of two fluorescence solutions attains the quantum values. The test specimen Φ can be calculated according the method employs well categorized standard samples to measure Φ_f.

Value of the standard sample Φ_f.

$$\Phi_f(U) = \frac{A_{std}}{A_u} \times \frac{S_u}{S_{std}} \times \left[\frac{n_u}{n_{std}}\right]^2 \times \Phi_{std}$$

Φ_{std} : Fluorescence quantum yield of standard/reference compound = 1

Φ_f (U) : Fluorescence quantum yield of unknown sample

n_{std} : Refractive index of the solvent in which standard compound was dissolved

A_{std} : Absorbance of the standard compound at a particular excitation wavelength

S_{std} : The total area of standard compound's emission spectrum

n_u : Refractive index of the solvent in which analyte sample was dissolved

A_u : Absorbance of the analyte sample at the same excitation wavelength applied for standard compound

S_u : The total area of analyte sample's emission spectrum

Φ_f of EA-PDI in $CHCl_3$

N,N′-bis(dodecyl)-3,4,9,10-perylenebis(discarboxiimide) was used as reference [23].

In $CHCl_3$, $\Phi_{std} = 1$

$A_{std} = 0.1055$

$A_u = 0.102$

$S_u = 10620.25$

$S_{std} = 4129.22$

$$\Phi_f = \frac{0.1055}{0.102} \times \frac{10620.25}{4129.22} \times \left[\frac{1.446}{1.446}\right]^2 \times 1$$

$\Phi_f = 0.72$

4.2 Molar Absorptivity (ε_{max}) Data of N,N′-Bis(1-methyl-2-cyanoethene)-3,4,9,10-perylenebis(dicarboxiimide) (EAPDI)

The following equation is utilized to find the molar absorptivity of the analyte samples.

$$\varepsilon_{max} = \frac{A}{Cl}$$

ε_{max} : Molar Absorptivity

A : absorbance in $mol \cdot L^{-1}$

c : solution's concentration (in $mol \cdot L^{-1}$)

l : the distance that light travel through the cell (in centimeters)

ε_{max} of EAPDI

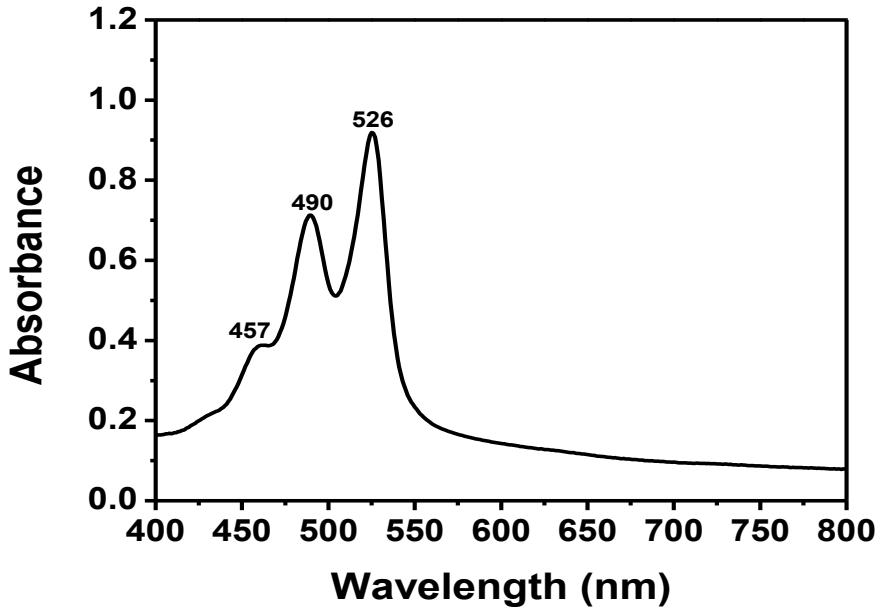

Figure 3.1: Absorption Spectrum of EAPDI in $CHCl_3$ at 1×10^{-5} M

From the Figure 4.1, the absorption is 0.92 at λ_{max} = 526nm.

⇨ $\varepsilon_{max} = \frac{0.92}{1\times10^{-5}M\times 1cm} = 92000$ L • mol^{-1} • cm^{-1}

⇨ ε_{max} of EAPDI = 92000 L • mol^{-1} • cm^{-1}

As shown representatively above, the ε_{max} of the compound (EAPDI) was estimated in three different solvents and the values were placed in Table 1.1.

Table1.1: Molar Aborptivity **(ε_{max})** Data of EAPDI in Different Solvents at 1×10^{-5} M

Name of Solvent	**Absorbance**	**λ_{max}**	**ε_{max} ($M^{-1}cm^{-1}$)**
DMF	0.792	524	79200
$CHCl_3$	0.92	526	92000
MeOH	0.393	521	39300

4.3 Full Width Half-Maximum ($\Delta\bar{\nu}_{1/2}$) Data Calculations

The half maximum of the full width 0→0 absorption band is the full width half maximum and can be calculated as below:

$$\Delta\bar{\nu}_{1/2} = \bar{\nu}_{I} - \bar{\nu}_{II}$$

Where, : $\bar{\nu}_{I}$, $\bar{\nu}_{II}$: The wavenumbers (inverted wavelengths) of the full width half maximum band (cm^{-1})

$\Delta\bar{\nu}_{1/2}$: Half-width of the 0→0 absorption band (cm^{-1})

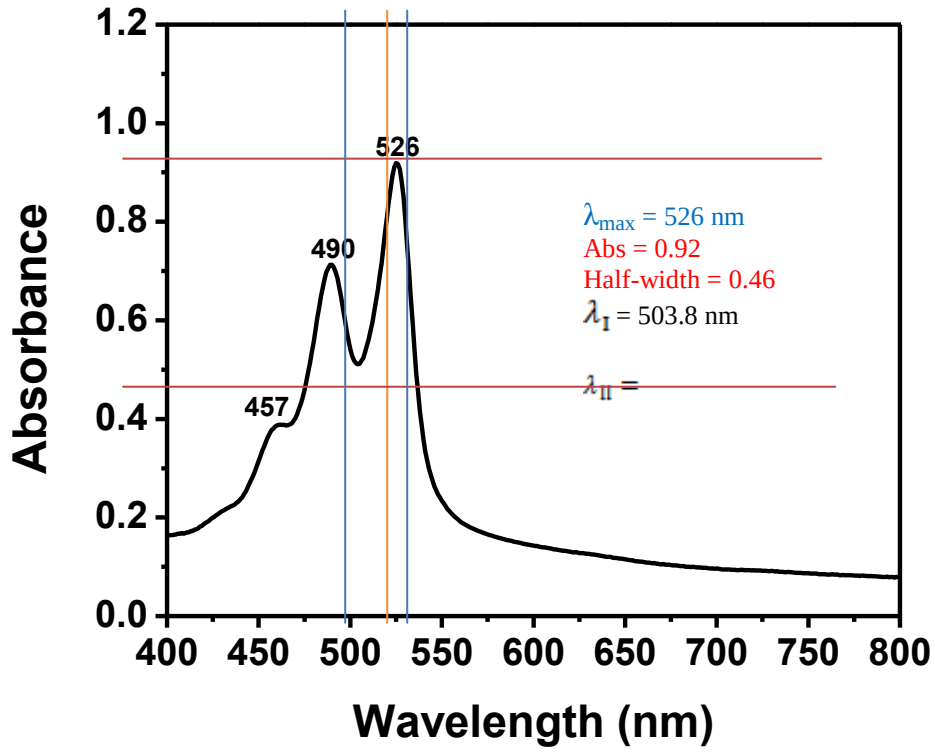

Figure 3.2 : Half Maximum of the Full Width 0→0 Absorption Band Representation from the Absorbance Spectrum of EAPDI in $CHCl_3$

According to Figure 4.2

λ_{max} = 526

Absorbance = 0.92

Half-width = 0.46

$\boldsymbol{\lambda_I}$ = 503.8 nm

$\boldsymbol{\lambda_{II}}$ = 537.5 nm

$$\Rightarrow \boldsymbol{\lambda_I} = 503.8 \text{ nm} \times \frac{10^{-9}\text{m}}{1\text{ nm}} \times \frac{1\text{cm}}{10^{-2}} = \mathbf{5.038 \times 10^{-5}\,cm}$$

$$\Rightarrow \bar{\nu}_I = \frac{1}{5.038 \times 10^{-5}\text{cm}} = \mathbf{19849\ cm^{-1}}$$

λ_{II} = 537.5 nm

$$\Rightarrow \boldsymbol{\lambda_{II}} = 537.5 \text{ nm} \times \frac{10^{-9}\text{m}}{1\text{ nm}} \times \frac{1\text{cm}}{10^{-2}} = \mathbf{5.375 \times 10^{-5}\,cm}$$

$\Rightarrow \boldsymbol{\lambda_{II}}$ = 5.375 = 18605 cm^{-1}

$\Delta\bar{\nu}_{1/2} = \bar{\nu}_I - \bar{\nu}_{II}$ = 19849 cm^{-1} – 18605 cm^{-1} = 1244 cm^{-1}

$\Rightarrow \boldsymbol{\Delta\bar{\nu}_{1/2}}$ = 1244 cm^{-1}

The half-width of the chosen absorptions of EAPDI in different solvents were measured in similar way and presented in Table 1.2.

Table 1.2: Half-width ($\Delta\bar{\nu}_{1/2}$) Values of the 0→0 Absorptions of EAPDI in Different Solvents at 1×10^{-5} M

Name of the Solvent	$\boldsymbol{\lambda_I}$**(nm)**	$\boldsymbol{\lambda_{II}}$ **(nm)**	$\boldsymbol{\Delta\bar{\nu}_{1/2}}$ **(cm^{-1})**
DMF	503.8	537.5	1244
$CHCl_3$	506.2	537.5	1150
MeOH	502.5	546.3	1596

4.4 Theoretical Radiative Lifetime Calculations (τ_0)

The radiative lifetime of a molecule shows to the lifetime of an active molecule theoretically calculated without nonradiative transitions.

$$\tau_0 = \frac{3.5\times10^8}{\bar{\nu}^2_{max}\times\varepsilon_{max}\times\Delta\bar{\nu}_{1/2}}$$

Where,

τ_0 : Theoretical radiative lifetime (ns)

$\varepsilon_{max.}$: Maximum molar absorptivity in L • mol^{-1} • cm^{-1} at λ_{max}

$\bar{\nu}_{max.}$: Inverted Mean Wavelength of the 0→0 absorption band (cm^{-1})

$\Delta\bar{\nu}_{1/2}$: Half-width values of the 0⟶0 absorptions (cm^{-1})

Theoretical radiative lifetime τ_0 of EAPDI:

By the calculated values from previous sections, (ε_{max} and $\Delta\bar{\nu}_{1/2}$) of nominated absorptions of EAPDI,

λ_{max} = 526

$$\lambda_{max} = 526\text{nm} \times \frac{10^{-9}\text{m}}{1\text{ nm}} \times \frac{1\text{cm}}{10^{-2}\text{ m}} = 5.26\times10^{-5}\text{cm}$$

$$\Rightarrow \bar{\nu}_{max} = \frac{1}{5.26\times10^{-5}\text{cm}} = 19011.40\ \text{cm}^{-1}$$

$$\Rightarrow \bar{\nu}^2_{max} = (19011.40\ \text{cm}^{-1})^2 = 3.614\times10^8\ \text{cm}^{-2}$$

Now, the theoretical base of radiative lifetime of EAPDI is measured according to the previous equation.

$$\tau_0 = \frac{3.5\times10^8}{\bar{\nu}^2_{max}\times\varepsilon_{max}\times\Delta\bar{\nu}_{1/2}} = \frac{3.5\times10^8}{(19011.40)^2\times92000\times1150}$$

⇨ $\tau_0 = 9.2\times10^{-9}$ s

⇨ τ_0 = 9.2 ns

Likewise, the theoretical radiative lifetimes of EAPDI in different solvents were measured and given in Table 1.3.

Table 1.3: Theoretical Radiative Lifetime **(τ_0)** of EAPDI in Different Solvents at 1×10^{-5} M

Name of the Solvent	**ε_{max}** **($M^{-1}cm^{-1}$)**	**$\Delta\bar{\nu}_{1/2}$** **(cm^{-1})**	$\bar{\nu}^2_{max}$ cm^{-2}	**τ_0(ns)**
DMF	79200	1244	3.64×10^8	9.8
$CHCl_3$	92000	1150	3.6×10^8	9.2
MeOH	39300	1596	3.68×10^8	23

4.5 Theoretical Fluorescence Lifetime Calculations (τ_f)

Applying the equation mentioned below, the theoretical fluorescence lifetime was calculated for EAPDI. This shows the theoretical time average of the EAPDI molecule spent in the excited state before fluorescence.

$$\tau_f = \tau_0 \cdot \Phi_f$$

Where,

τ_f : Fluorescence lifetime in nano seconds

τ_0 : Theoretical radiative lifetime in nano seconds

Φ_f : Fluorescence quantum yield

$$\tau_f = \tau_0 \cdot \Phi_f$$

$= 9.2 \times 0.72$

$\tau_f = 6.624$ ns

4.6 Calculations of Theoretical Fluorescence Rate Constant (k_f)

The theoretically determined rate constant of fluorescence of the compounds is measured through the formula:

$$k_f = \frac{1}{\tau_0}$$

Where,

k_f : Theoretically determined rate constant of fluorescence in s^{-1}

τ_0: Theoretical radiative lifetime in nano seconds in s

k_f of EAPDI in $CHCl_3$:

$$k_f = \frac{1}{9.2\times 10^{-9}} = 10.87 \times 10^7$$

The theoretically determined rate constant of fluorescence were measured likely as represented above in few solvents and tabulated.

Table 1.4: Theoretically Determined Rate Constant of Fluorescence (k_f) of EAPDI in Different Solvents at 1×10^{-5} M

Name of the Solvent	**τ_0 (ns)**	**k_f**
DMF	9.8	10.87×10^{-7}
$CHCl_3$	9.2	10.20×10^{-7}
MeOH	23	4.35×10^{-7}

4.7 Oscillator Strength Calculations (f)

The oscillator strength is a dimensionless quantity infers the of strength of an electronic transition. It can be calculated according to the give below equation:

$$f = 4.32 \times 10^{-9}\, \Delta\bar{\nu}_{1/2} \times \varepsilon_{max}$$

f : Oscillator strength

$\Delta\bar{\nu}_{1/2}$: Half-width Values of the 0→0 Absorptions (cm^{-1})

$\varepsilon_{max.}$: maximum molar absorptivity in L • mol^{-1} • cm^{-1} at maximum wavelength (λ_{max})

The strength of electronic transition (f) of EAPDI

⇨ $f = 4.32 \times 10^{-9} \times \Delta\bar{\nu}_{1/2}\, \varepsilon_{max}$

⇨ $f = 4.32 \times 10^{-9} \times 1150 \times 92000$

⇨ $f = 4.57 \times 10^{-1}$

Oscillator strength of radiationless deactivation for EAPDI in different solvents shows in Table 1.5.

Table 1.5: The Oscillator Strength (f) of Electronic Transition Data of EAPDI Estimated in Different Solvents at 1×10^{-5} M

Name of the Solvent	$\Delta\bar{\nu}_{1/2}$ **(cm^{-1})**	ε_{max} **($M^{-1}cm^{-1}$)**	f
DMF	1244	79200	0.425
$CHCl_3$	1150	92000	0.457
MeOH	1596	39300	0.271

4.8 Singlet Energy Calculations (E_s)

Singlet energy is the necessary amount of energy for electronic transitions from the ground state to an excited electronic state.

$$E_s = \frac{2.86 \times 10^5}{\lambda_{max}}$$

E_s : The Singlet energy in (kcal . mol^{-1})

λ_{max} : The maximum absorption wavelength in $\overset{o}{A}$

Singlet Energy of EAPDI:

$$E_s = \frac{2.86 \times 10^5}{\lambda_{max}} = \frac{2.86 \times 10^5}{5260} = 54.37 \text{ kcal .mol}^{-1}$$

E_s = 54.37 kcal . mol^{-1}

The singlet energies of EAPDI were calculated in different solvents similarly as shown above and were presented in the Table 1.6

Table 1.6: Singlet Energy (E_s) Data of EAPDI in Different Solvents at 1×10^{-5} M

Name of the Solvent	λ_{max}	E_s **(kcal . mol^{-1})**
DMF	5240	54.58
$CHCl_3$	5260	54.37
MeOH	5210	54.89

4.9 Calculations of Optical Band Gap Energies (E_g)

The optical band gap energy provides significant data about its HOMO and LUMO energy states which are important concerning solar cells.

$$E_g = \frac{1240 \text{ eV nm}}{\lambda}$$

Where,

E_g : Energy of band gap in electron volts (eV)

λ : The wavelength that cut-off of the 0 → 0 absorption band in nm

E_g of EAPDI:

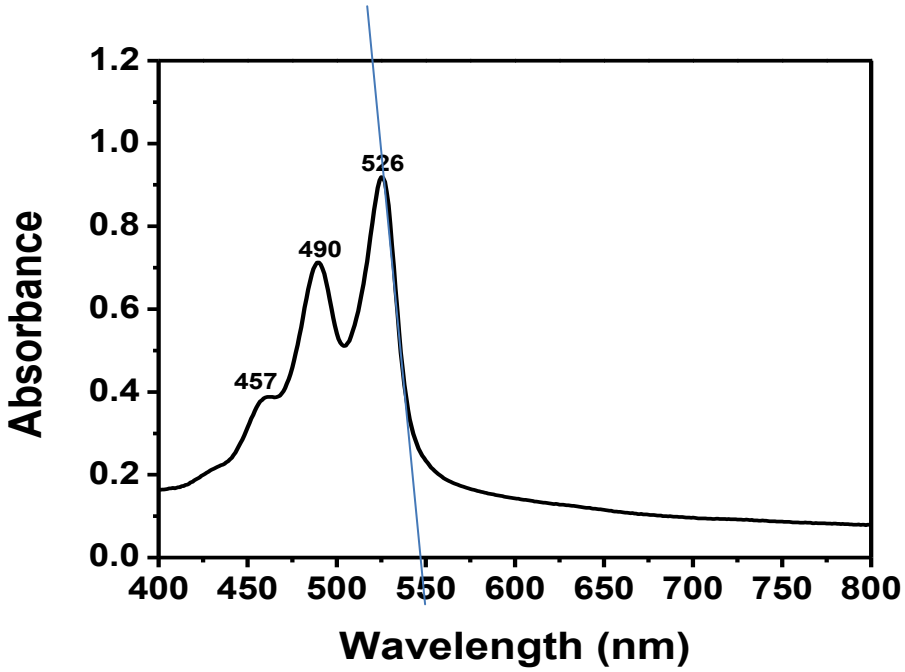

Figure 3.3: Absorption Spectrum of EAPDI in Different Solvents and the Cut-off Wavelength

$$E_g = \frac{1240\ \text{eV nm}}{\lambda}$$

$$E_g = \frac{1240\ \text{eV nm}}{\lambda} = \frac{1240\ \text{eV nm}}{\lambda} = 2.26$$

$E_g = 2.26\ eV$

Table 1.7: Data of Band Gap Energies of EAPDI in Different Solvents at 1×10^{-5} M

Name of the Solvent	**Wavelength that Cut-off**	E_g**(eV)**
DMF	552.5	2.24
$CHCl_3$	547.7	2.26
MeOH	556.3	2.23

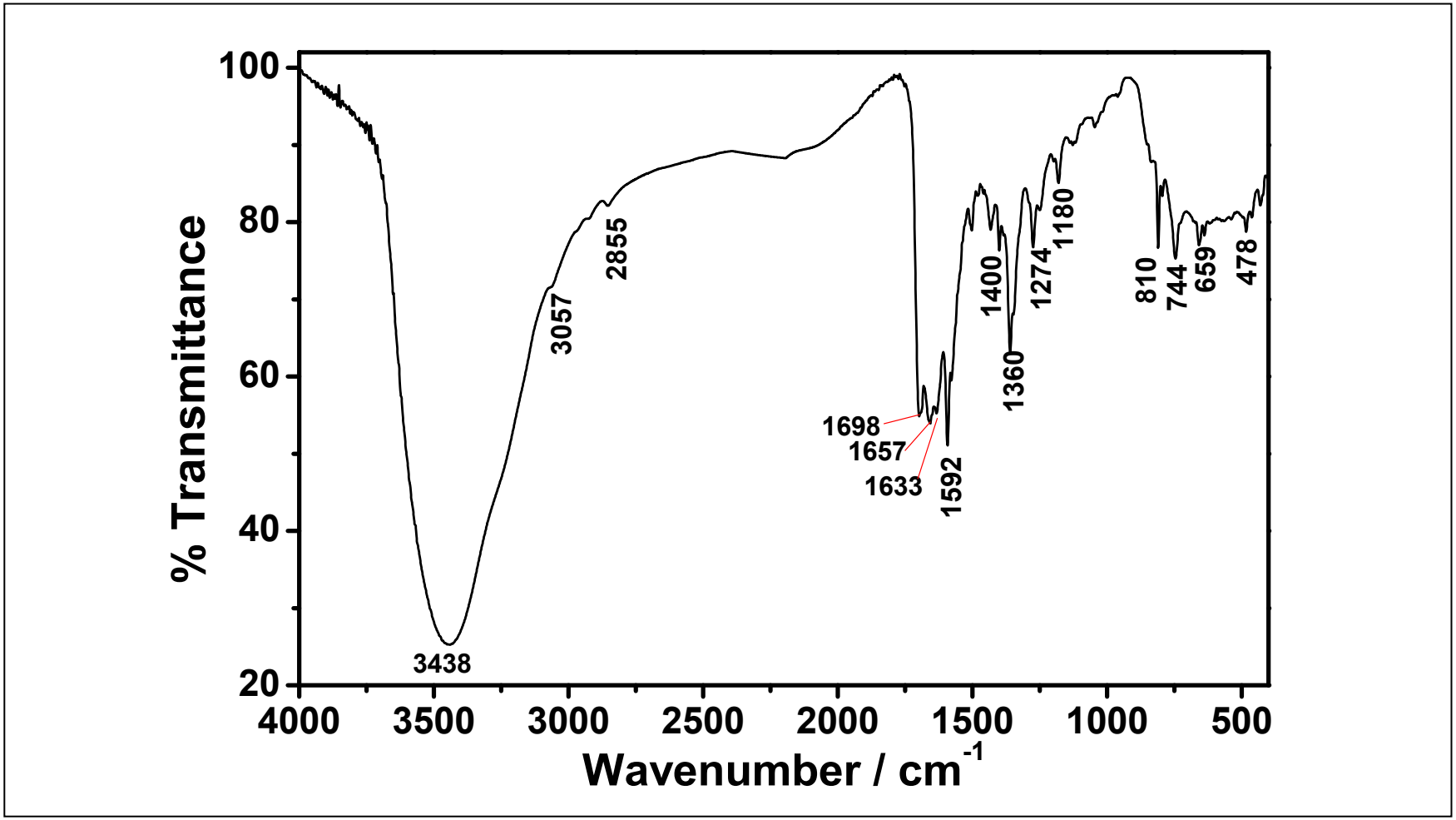

Figure 3.4: Infrared (Fourier Transform Infrared) Spectrum of EAPDI

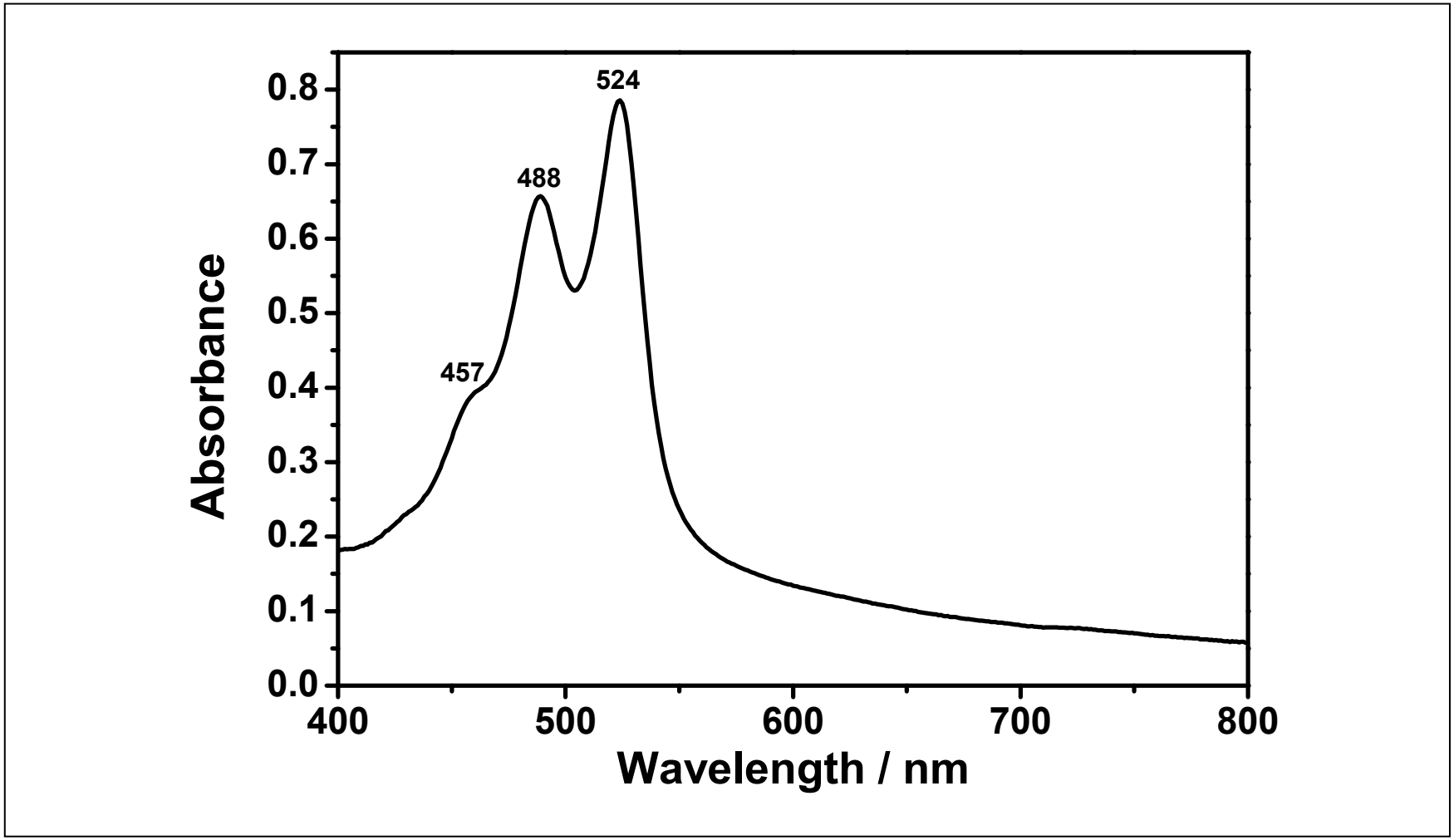

Figure 3.5: Absorption Spectrum of EAPDI in DMF

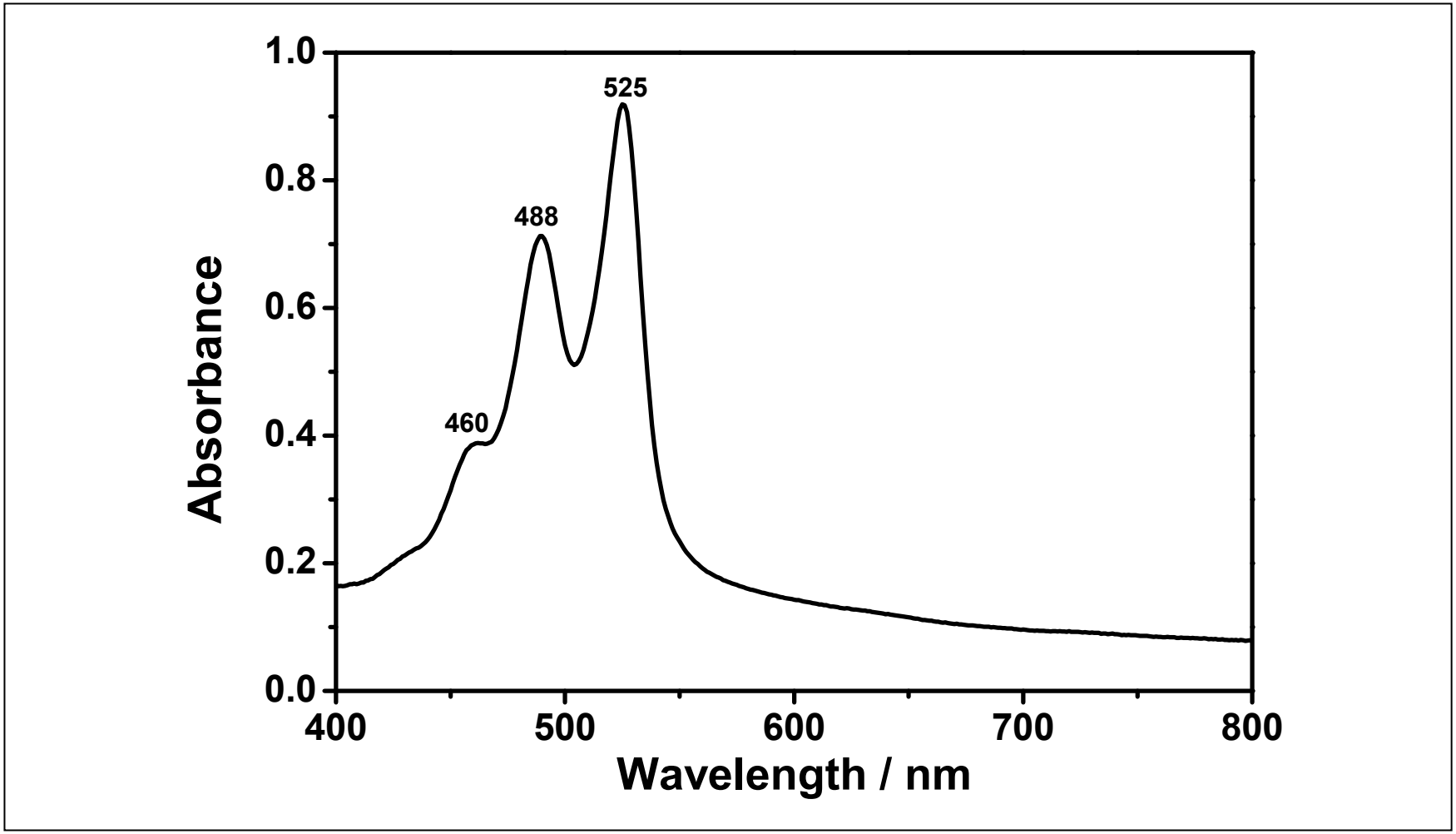

Figure 3.6: Absorption Spectrum of EAPDI in $CHCl_3$

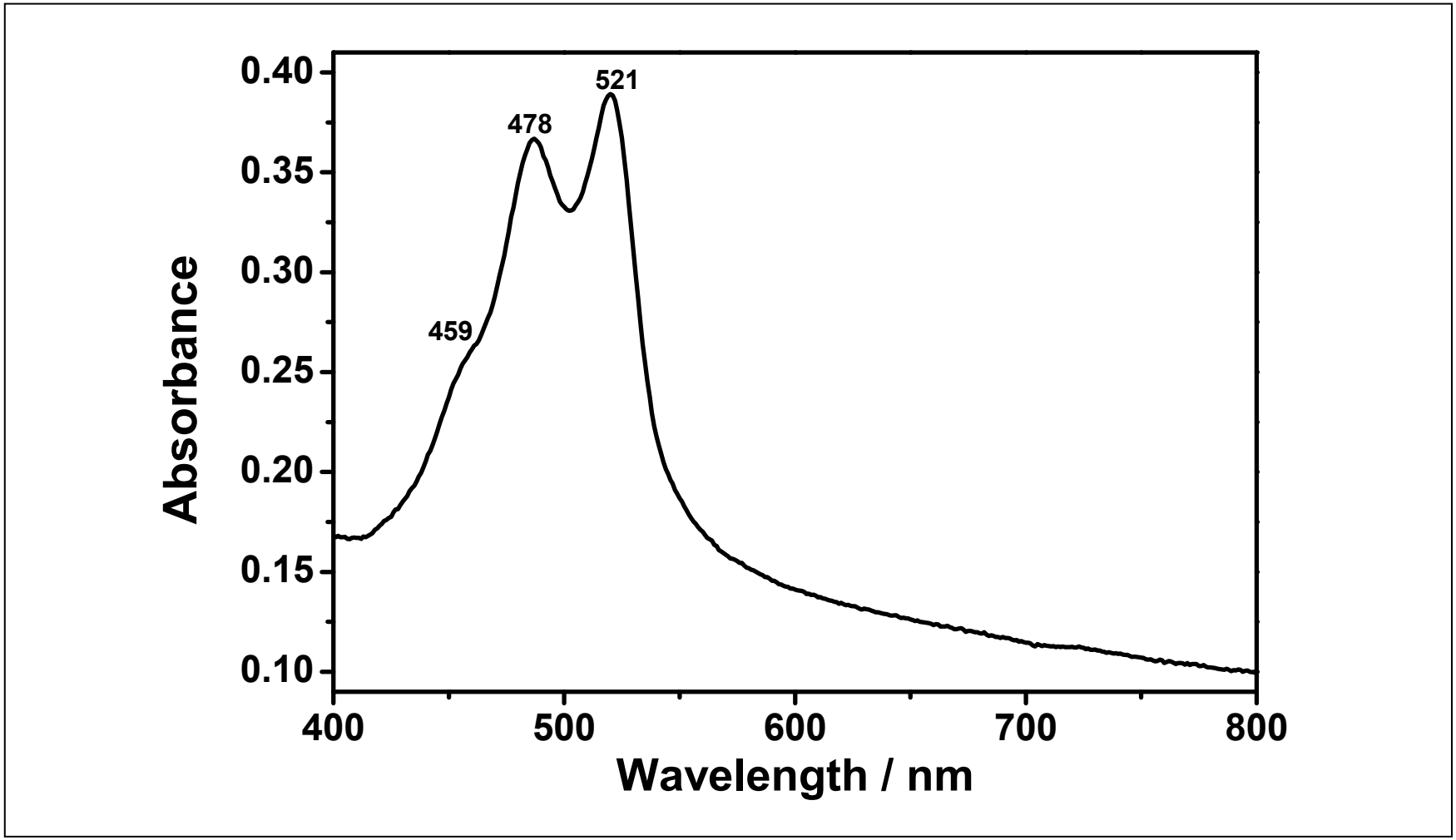

Figure 3.7: Absorption Spectrum of EAPDI in CH_3OH

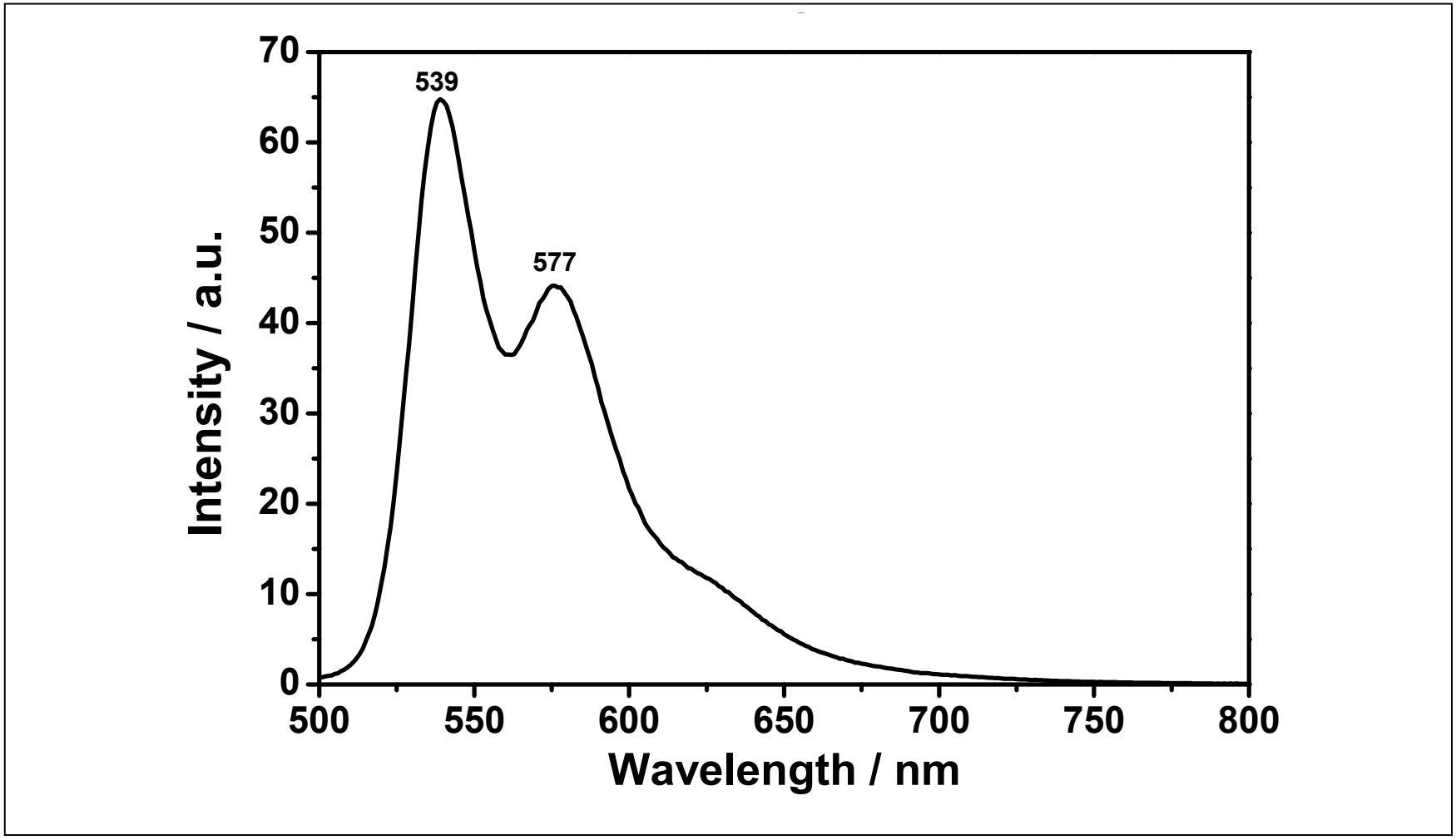

Figure 3.8: Emission Spectrum of EAPDI in DMF

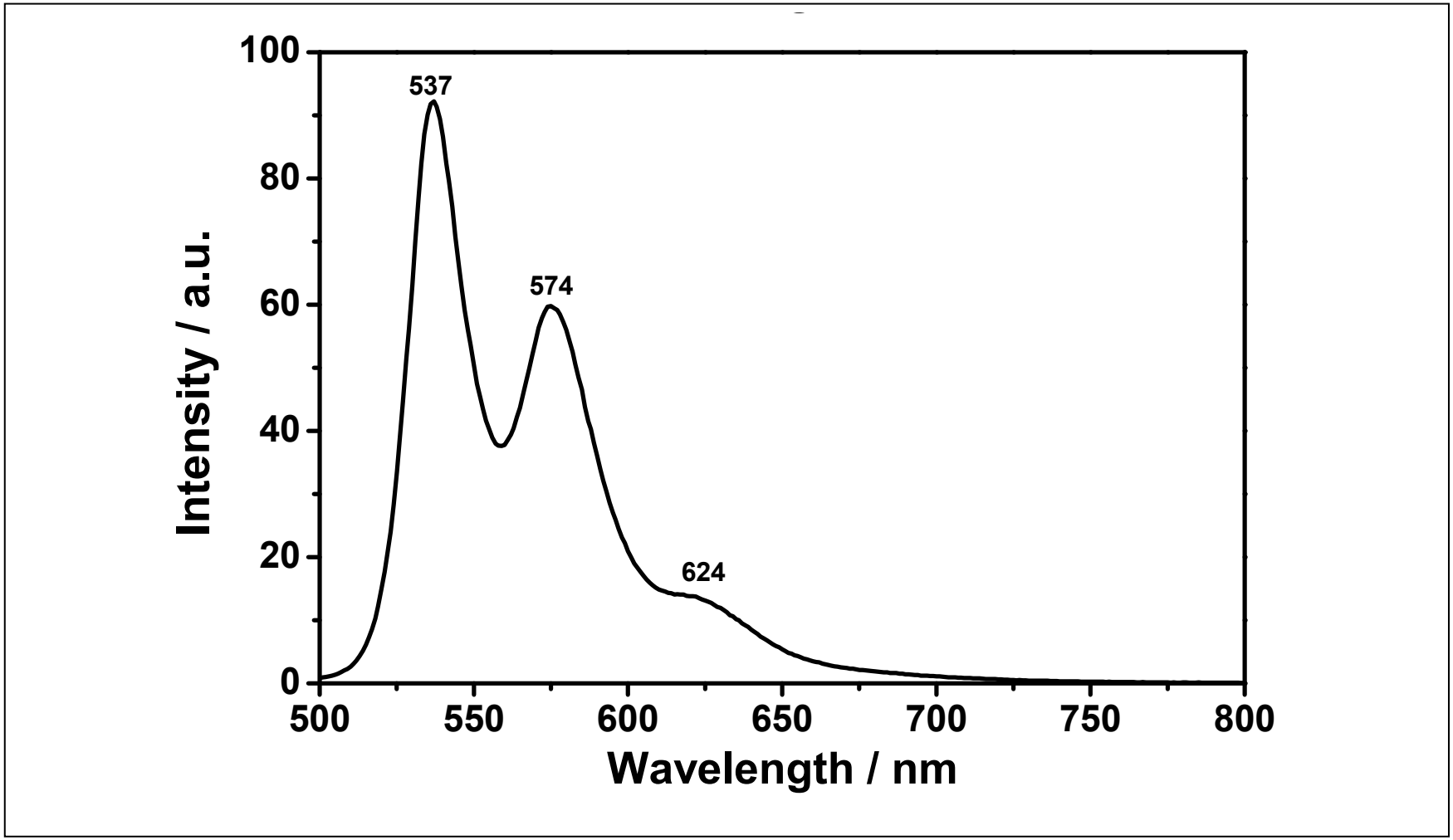

Figure 3.9: Emission Spectrum of EAPDI in $CHCl_3$

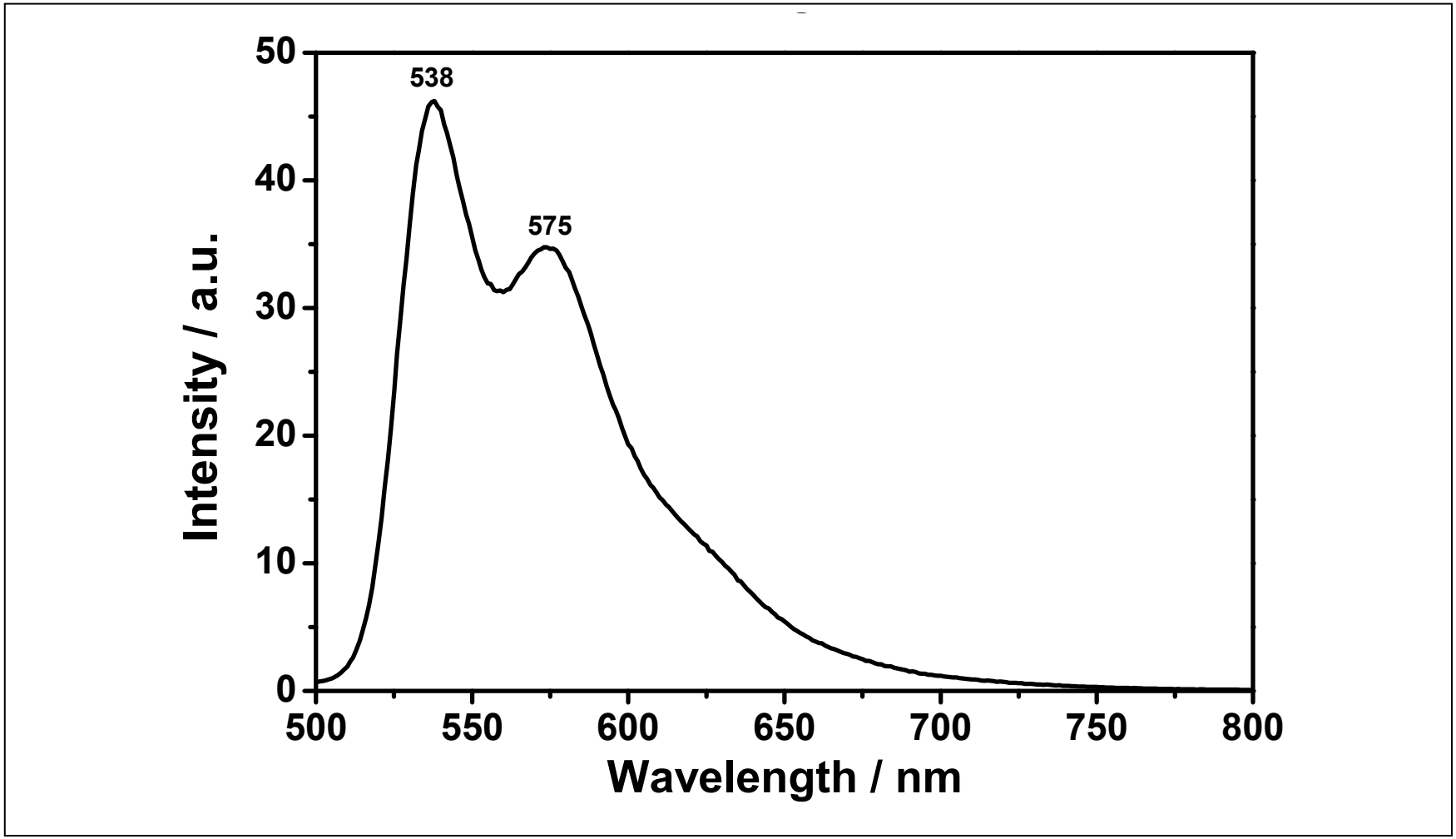

Figure 3.10: Emission Spectrum of EAPDI in CH_3OH

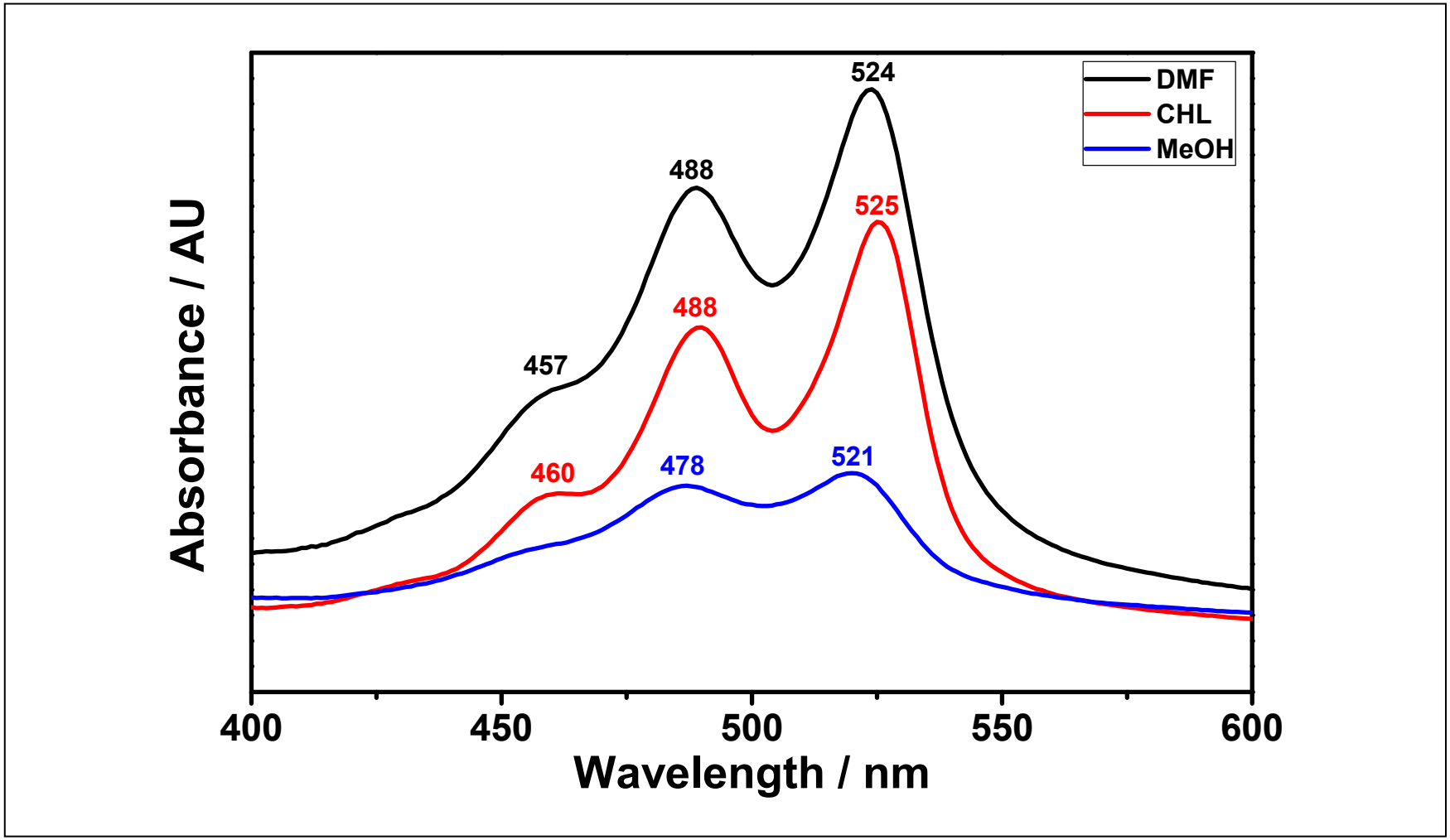

Figure 3.11: Absorption Spectra of EAPDI in Different Solvents: DMF, $CHCl_3$, CH_3OH

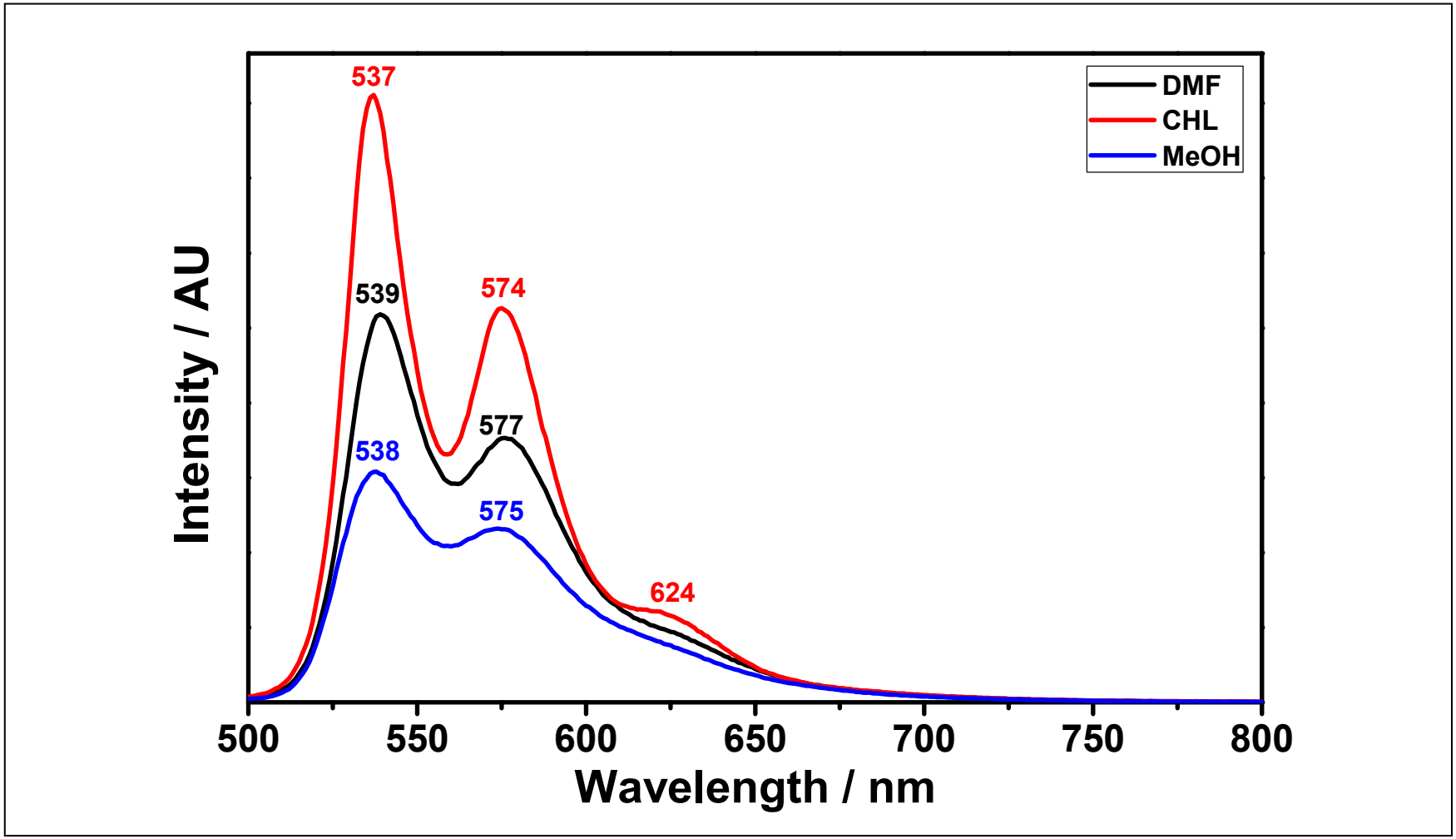

Figure 3.12: Emission Spectra of EAPDI in Different Solvents: DMF, $CHCl_3$, CH_3OH

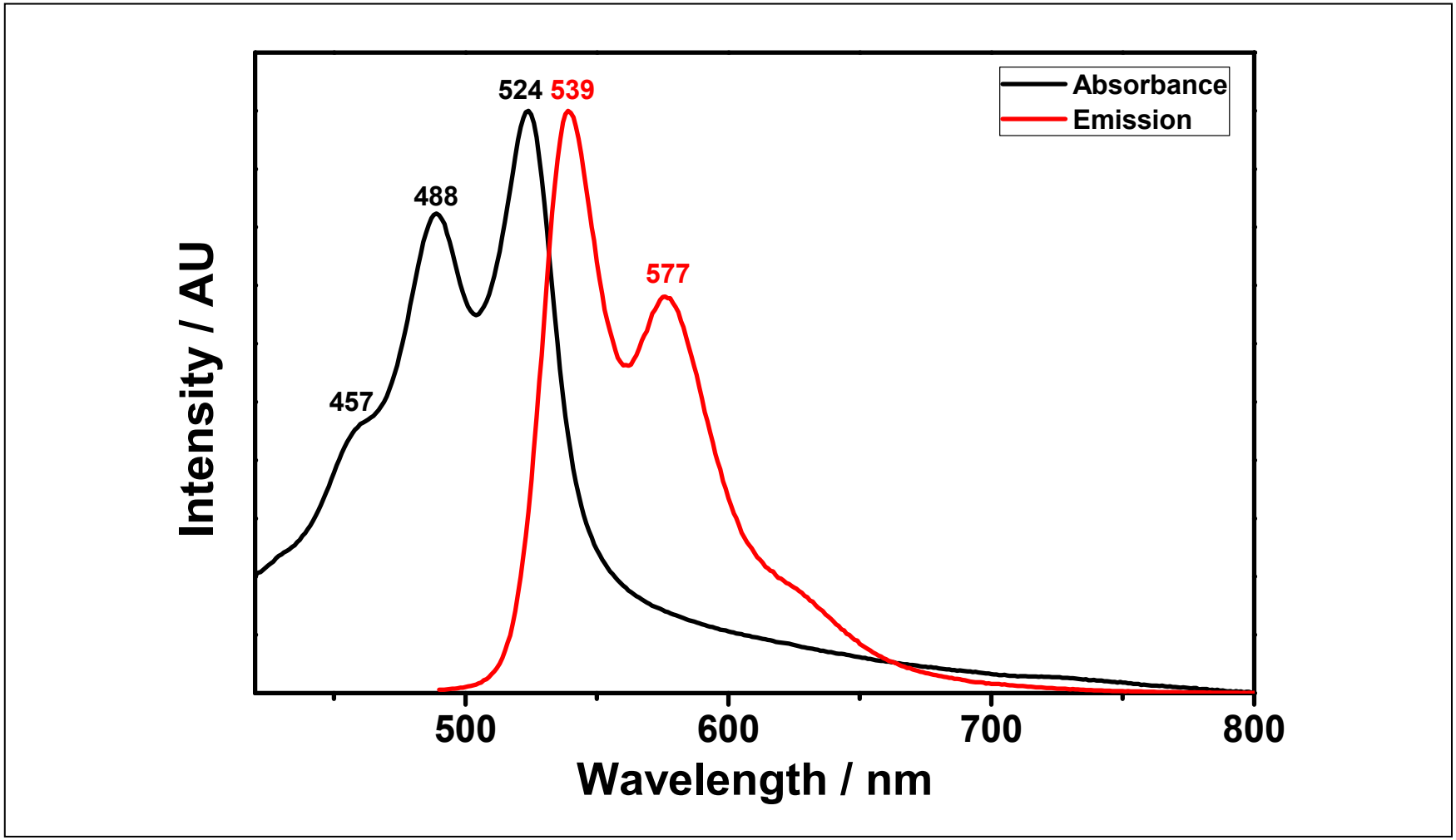

Figure 3.13: Mirror Image Spectra of Absorption and Emission of EAPDI in Solvent, DMF

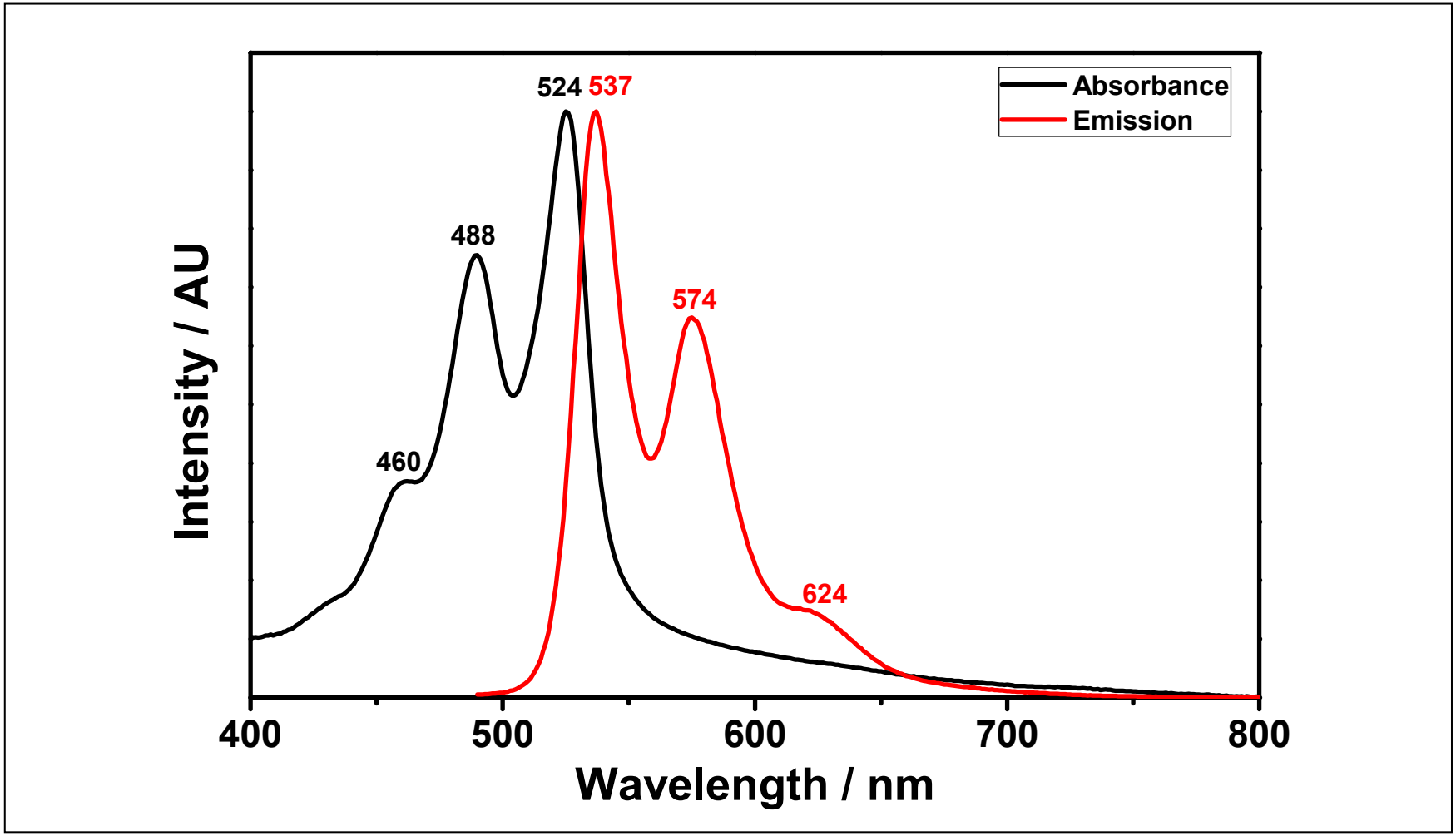

Figure 3.14: Mirror Image Spectra of Absorption and Emission of EAPDI in Solvent, $CHCl_3$

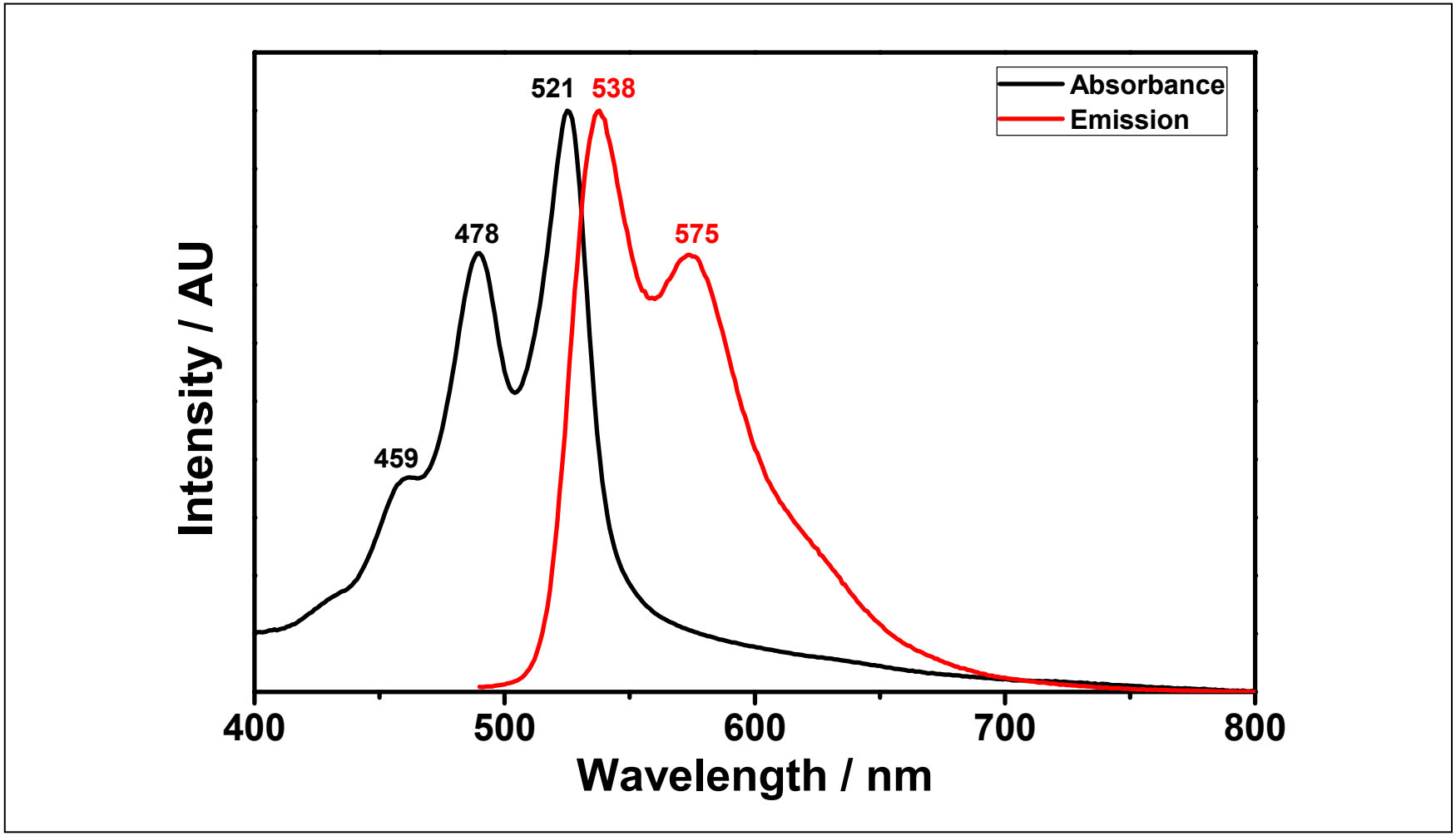

Figure 3.15: Mirror Image Spectra of Absorption and Emission of EAPDI in Solvent, CH_3OH

Chapter 5

RESULTS AND DISCUSSION

5.1 Synthesis of N,N′-Bis(1-methyl-2-cyanoethene)-3,4,9,10-perylenebis (dicarboxiimide) (EAPDI)

A new electron accepting perylenebisimide N,N′-bis(1-methyl-2-cyanoethene)-3,4,9,10-perylenebis(dicarboxiimide) (EAPDI) was efficiently synthesized. An aliphatic substituent is presented at imide regions to increase the solubility, and to improve the electrochemical and optical properties of the perylene bisimide.

The synthesized bisimide EAPDI was characterized by FT-IR spectroscopy and its photophysical properties were studied by UV–vis and emission techniques.

5.2 Solubility of the Synthesized Perylene Dye

The N,N′-bis(1-methyl-2-cyanoethene**)**-3,4,9,10-perylenebis(dicarboxiimide) is completely soluble in dipolar aprotic solvents DMF, but partially soluble in both of polar protic solvent methanol, and in nonpolar solvent $CHCl_3$. Table 5.1 shows solubility properties of EAPDI in different solvents.

Table 5.1: Solubility of EAPDI in Different Solvents

Solvent	**EAPDI**	**Color**
DMF	(+ +)	Light purple
$CHCl_3$	(– +)	Light purple
MeOH	(– +)	Light purple

(+ +) soluble at room temperature; (– +) partially soluble.

5.3 Analysis of FT-IR Spectra

The synthesized perylenebisimide N,N′-bis(1-methyl-2-cyanoethene**)**-3,4,9,10-perylenebis(dicarboxiimide) EAPDI was basically characterized by FT-IR spectra in order to approve all the functional groups in their structure. The peaks which are observed by the FT-IR spectra are explained as following.

Figure 4.4, aromatic–CH stretching at 3057 cm^{-1}, aliphatic–CH stretching at 2855 cm^{-1}, imide C=O stretching at 1698 and 1657 cm^{-1}, conjugation of Ar C=C stretching at 1592, –C–N– stretching at 1360 cm^{-1}, Ar–CH bend at 810 cm^{-1} and 744 cm^{-1} approve the EAPDI's structure.

5.4 Analyses of UV-vis Absorption Spectra

From Figure 4.5 the absorption spectra of N,N′-bis(1-methyl-2-cyanoethene**)**-3,4,9,10-perylenebis(dicarboxiimide) EAPDI in highly polar aprotic solvent, DMF exhibits three characteristic UV-vis absorbtion bands at 457, 488 and 524 nm, respectively. It is belonging to perylene chromophoric $\pi \rightarrow \pi^*$ electronic transitions absorption. The three characteristic UV-vis absorption bands represent $0 \rightarrow 2$, $0 \rightarrow 1$, and $0 \rightarrow 0$ transitions of perylene chromophore, respectively.

Figure 4.6 demonstrates the UV-vis absorbance of EAPDI in non-polar solvent, $CHCl_3$. The spectrum illustrates three characteristic UV-vis absorbtion bands at 460, 488 and 525 nm, respectively. The $0 \rightarrow 0$ electronic transition is high in intensity that refers gradual increase in the absorption intensity. These three characteristic absorption peaks are associated with conjugated perylene chromophoric $\pi \rightarrow \pi^*$ interactions.

Figure 4.7 displays the UV-vis absorbance of EAPDI in polar protic solvent, methanol. The spectrum refers to UV-vis absorbtion bands at 459, 478 and 521 nm, respectively. There is no aggregation noticed. The $0 \rightarrow 0$ electronic transition peak at 521 nm is higher in absorption . Otherwise, EAPDI refers the lowest intensity at ground vibrational $0 \rightarrow$ singlet excited vibrational 2 electronic transition.

The comparison among UV-vis absorption spectra of EAPDI in dipolar aprotic solvent, DMF, non polar solvent, $CHCl_3$ and in polar protic solvent, CH_3OH shows a blue (hypsochromic) shift in polar protic solvent, MeOH because of hydrogen bonding (Figure 4.11).

5.5 Analyses of Emission Spectra

Figure 4.8 shows the emission spectrum (λ_{exc} = 485 nm) of N,N′-bis(1-methyl-2-cyanoethene)-3,4,9,10-perylenebis(dicarboxiimide), EAPDI in polar aprotic solvent, DMF. It displays two characteristic emission peaks of perylene chromophore at 539 and 577nm, respectively.

In nonpolar solvent, $CHCl_3$, EAPDI has shown three characteristic emission bands (λ_{exc} = 485 nm) at 537, 574 and 624 nm (Figure 4.9). The three emission peaks represent the 0→0, 1→0, and 2→0 electronic transitions of perylene chromophore and the highest intensity at 537 nm, whereas the lowest intensity at 624 nm. The absorption and emission spectra are mirror images of each other (Figure 4.14).

In polar and protic solvent, CH_3OH, N,N′-bis(1-methyl-2-cyanoethene)-3,4,9,10-perylenebis(dicarboxiimide), EAPDI has shown two emission spectra (λ_{exc} = 485 nm) at 538 and 575 nm (Figure 4.10). The highest intensity at 538 nm, while the lowest intensity at 575 nm.

The comparison made for absorption and emission spectra of EAPDI in dipolar aprotic solvent, DMF, non polar solvent, $CHCl_3$ and in polar protic solvent, CH_3OH were sown in Figures 4.11 and 4.12.

Figure 4.13-4.15 shows the overlap of absorption and emission spectra of EAPDI and the Stocks' shift in dipolar aprotic, DMF, nonpolar, $CHCl_3$ polar protic, CH_3OH. The absorbance and emission spectra in three types of solvents were mirror images of each other with Stocks' shifts of 15 nm, 13 nm, 17 nm, respectively.

Chapter 6

CONCLUSION

The novel N-substituted perylene bisimide N,N′-Bis(1-methyl-2-cyanoethene)-3,4,9,10-perylenebis(dicarboxiimide) (EAPDI) was synthesized successfully. An aliphatic substituent was introduced at imide regions by the condensation reaction between PDA and 3-aminocrotononitrile to increase the solubility, and to improve the electrochemical and optical properties of the perylene bisimide.

The compound was purified and the resulting EAPDI was characterized by FT-IR to confirm the structure with its functional groups . The photo physical properties of EAPDI were studied through UV-vis and emission techniques.

The UV-vis absorption spectra of EAPDI display three characteristic absorption bands. Also EAPDI has shown three traditional emission peaks in all of the reported organic solvents. The emission spectra of EAPDI or the mirror image of its absorption spectra with a varying stokes shift between 13 nm and 17 nm.

The prepared EAPDI has shown perfect solubility in the dipolar aprotic solvent.

REFERENCES

[1] Al-Hussein, M., Hesse,H.C., Weickert, J., Dössel,L., Feng, & X., Schmidt, L, M. (2011). Structural properties of the active layer of discotic hexabenzocoronene perylene diimide bulk hetero junction photovoltaic devices: The role of alkyl side chain length. *Thin Solid Films*. 520, 307–313.

[2] Chai,S., HaoWena, S., & Li Han, K. (2011). Understanding Electron-Withdrawing Substituent Effect on Structural, Electronic and Charge Transport Properties of perylene Bisimide Derivatives.*Organic Electronics*. 12, 1806–1814.

[3] Dentani, T., Funabiki, K., Jin, J. Y., Yoshida,T., Minoura., H., & Matsui, M. (2007). Application of 9-substituted 3, 4-perylenedicarboxylic anhydrides as sensitizers for zinc oxide solar cell. *Dyes and pigments*. 72, 303–307.

[4] Fortage, j., S´everac, M., Rassin, C. H., Pellegrin, Y., Blart, E., & Odobel, F. (2008). Synthesis of new perylene imide dyes and their photovoltaic performances in nanocrystalline TiO_2 dye-sensitized solar cells. *Journal of Photochemistry and Photobiology A: Chemistry*.197, 156–169.

[5] Georgiev, N. I., Sakr, A. R., & Bojinov, V. B. (2011). Design and Synthesis of Novel Fluorescence Sensing Perylene Diimides Based on Photoinduced Electron Transfer. *Dyes and Pigment*s. 91, 332–339.

[6] Grätzel, M. (2003). Dye-sensitized solar cells. *Journal of Photochemistry and Photobiology C: Photochemistry Reviews*. 4, 145–153.

[7] Grätzel, M. (2005). Solar energy conversion by dye-sensitized photovoltaic cells. *Inorganic chemistry*. 44, 6841–6851.

[8] Hui Luo, M., & Yu Chen, K. (2013). Asymmetric PeryleneBisimide Dyes with Strong Solvatofluorism. *Dyes and Pigments.* 99, 456–464.

[9] Howard, I. A., Meister, M., Baumeier, B., Wonneberge, H., Pschirer, N., Sens, R., Bruder, I., Li, C., Müllen, K., Andrienko, D., &Laquai, F. (2013). Two Channels of Charge Generation in PeryleneMonoimide Solid–State Dye-Sensitized Solar Cells. *Advanced Energy Materials*. 10, 1–8.

[10] Jung, M., Baston, U., Schnitzle, G., Kaiser, M., Papst, J., Porwol, T., Freund, H. J., & Urnbac, E. (1993). The electronic structure of adsorbed aromatic molecules: Perylene and PTCDA on Si (111) and Ag (111). *Journal of Molecular Structure*. 293, 239–244.

[11] Kozma¸ E., Kotowski¸ D., Catellani, M., Catellani¸ S., Famulari¸ A., & Bertini, F. (2013). Synthesis and Characterization of New Electron Acceptor Perylene Diimide Molecules for Photovoltaic Applications. *Dyes and Pigments*. 99, 329–338.

[12] Karlsson, M. (2012). Materials Development for Solid-state Dye-Sensitized Solar Cells. Phd Thesis, Acta Universitatis Upsaliensis Uppsala.

[13] Li,C., & Wonneberger, H. (2012). Perylene Imides for Organic Photovoltaics: Yesterday, Today, and Tomorrow. *Advanced Mateialsr*. 24, 613–636.

[14] Lukas, S. A., Zhao, Y., Miller, S. E., & Wasielewski, M. R. (2002). Biomimetic electron transfer using low energy excited states: A green perylene-based analogue of chlorophyll a. *The Journal of Physical Chemistry B*. 106, 1299–1306.

[15] Li, G., Shrotriyal,V., Huangl, J., yaol, Y., Moriarty, T., Emery, K., & Yang, Y. (2005). High-efficiency solution processable polymer photovoltaic cells by self-organization of polymer blends. *Nature materials*. 4, 864–868.

[16] Li, C., Schçneboom, J., Liu, Z., Pschirer, N. G., Erk, P., Herrmann, A., & Mullen, K,. (2009). Rainbow perylene monoimides: easy control of optical properties. *Chemistry European Journal.*15, 878–884.

[17] Lang, L. S., Muth, M.A., Heinrich, C, D., Orozco, M,C., Thelakkat, M. (2013). Pendant Perylene Polymers with High Electron Mobility. *Journal of Polymer Science*. 51, 1480–1486.

[18] Sharma,G. D., Roy, M. S., Mikroyannidis, J. A., & Justin Thomas, K. R. (2012). Synthesis and Characterization of a New PeryleneBisimide (PBI) Derivative and its Application as Electron Acceptor for Bulk Heterojunction Polymer Solar Cells. *Organic Electronics.*13, 3118–3129.

[19] Shibano, Y., Umeyama, T., Matano, Y., Tkachenko, N. V., Lemmetyinen, H., Araki, Y., Ito, O., & Imahori, H. (2007). Large reorganization energy of pyrrolidine-substituted perylenediimide in electron transfer. *The Journal of Physical Chemistry C*. 111,16, 6133–6142.

[20] Wang, S., Li, Y., Du, C., Shi, Z., Xiao, S., Zhu, D., Gao, E., & Cai, S. (2002). Dye sensitization of nanocrystalline TiO_2 by perylene derivatives. *Synthetic Metals.*128, 299–304.

[21] Zhou, E., Cong, J., Wei, Q., Tajima, K., Yang, C., &Hashimoto, K. (2011). All-Polymer Solar Cells from PeryleneDiimide Based Copolymers: Material Design and Phase and Separation Control. *Angew.Chem. Int. Ed*. 50, 2799–2803.

[22] Zafer, C,. Kus, M., Turkmen, G., Dincalp, H., Demic, S., Kuban,B., Yildirim, T., & Icli, S. (2007). New perylene derivative dyes for dye-sensitized solar cells. *Solar energy materials and solar cells*. 91, 427–431.

[23] Icil, H., & Icili, S. (1997). Synthesis and Properties of a New Photostable Polymer: Perylene-3,4,9,10-tetracarboxylic Acid–bis-(N,N'-dodecylpolyimide). *Journal of Polymer Science Part A: Polymer Chemistry*. 35, 2137–2142.